

CrystEngComm

Accepted Manuscript



This is an *Accepted Manuscript*, which has been through the Royal Society of Chemistry peer review process and has been accepted for publication.

Accepted Manuscripts are published online shortly after acceptance, before technical editing, formatting and proof reading. Using this free service, authors can make their results available to the community, in citable form, before we publish the edited article. We will replace this *Accepted Manuscript* with the edited and formatted *Advance Article* as soon as it is available.

You can find more information about *Accepted Manuscripts* in the [Information for Authors](#).

Please note that technical editing may introduce minor changes to the text and/or graphics, which may alter content. The journal's standard [Terms & Conditions](#) and the [Ethical guidelines](#) still apply. In no event shall the Royal Society of Chemistry be held responsible for any errors or omissions in this *Accepted Manuscript* or any consequences arising from the use of any information it contains.

Syntheses, structures, luminescence and molecular recognition properties of four new cadmium carboxyphosphonates with 2D layered and 3D supramolecular structure

Lu-Lu Dai, Yan-Yu Zhu, Cheng-Qi Jiao, Zhen-Gang Sun,* Shao-Ping Shi, Wei Zhou, Wen-Zhu Li, Tong Sun, Hui Luo and Ming-Xue Ma

School of Chemistry and Chemical Engineering, Liaoning Normal University, Dalian 116029, P. R. China

Four new cadmium carboxyphosphonates with 2D layered and 3D supramolecular structure, namely, $\text{Cd}_3[(4\text{-cppH})_2(4\text{-cppH}_2)_2]$ (**1**), $\text{Cd}[(2,2'\text{-bipy})(4\text{-cppH})]$ (**2**), $[\text{Cd}_3(1,10\text{-phen})_3(4\text{-cpp})_2]\cdot 6\text{H}_2\text{O}$ (**3**) and $[\text{Cd}(4,4'\text{-bipy})(4\text{-cppH})(\text{H}_2\text{O})_2]\cdot 2\text{H}_2\text{O}$ (**4**) (4-cppH₃ = 4-carboxyphenylphosphonic acid, 2,2'-bipy = 2,2'-bipyridine, 1,10-phen = 1,10-phenanthroline and 4,4'-bipy = 4,4'-bipyridine), have been synthesized under hydrothermal conditions. In compound **1**, {Cd(1)O₆}, {Cd(2)O₆}, {Cd(3)O₆} and {CPO₃} polyhedra form a layer in *ab* plane *via* edge- and corner-sharing. Neighboring layers compose into a 3D supramolecular network by hydrogen bonding interactions. The structure of compound **2** shows a new layered structure, in which the interconnection of two {Cd(1)O₄N₂} and two {CPO₃} polyhedra *via* corner-sharing forms a tetranuclear cluster, and the so-built tetranuclear clusters are bridged by the phosphonate ligands into a 2D layer. For compound **3**, {Cd(1)O₄N₂}, {Cd(2)O₄N₂}, {Cd(3)O₃N₂} and {CPO₃} polyhedra are interconnected by carboxyphosphonate ligands to a 2D layer in *ac* plane. Then the adjacent layers are further assembled into a 3D supramolecular structure through π - π stacking interactions. Cd(II) ions in compound **4** are bridged by 4,4'-bipy molecules into layers in *ab* plane. These layers are held together by hydrogen bonds into a 3D supramolecular structure. The thermal stabilities and luminescence properties of compounds **1–4** have been investigated. Interestingly, compound **1** is selective and reversible for sensing of DMF and acetone.

Introduction

The chemistry of metal phosphonates has been an active research field over the past years, mainly due to their compositional and structural diversities, as well as potential applications in the areas of catalysis, magnetism, ion exchanging, porous materials, photochemistry, and materials chemistry.¹ At least three approaches can be employed in order to obtain these materials by (1) using phosphonate ligands with additional functional groups; (2) introducing a second inorganic or organic ligand to the system; (3) using different templates or mineralizers in the reaction mixture.²

* To whom correspondence should be addressed: E-mail: szg188@163.com

During the past few years, many metal phosphonates have been prepared through designing and synthesizing phosphonic acids containing $-\text{NH}_2$, $-\text{OH}$, and $-\text{COOH}$ sub functional groups and providing many coordination modes. The introduction of additional organic functional groups to the phosphonate ligands would result in compounds with not only novel structures but also interesting properties.³ By attaching functional groups such as amine, hydroxyl, and carboxylate groups to the phosphonic acid, a series of metal phosphonates with different architectures have been isolated in our laboratory.⁴ Another important and useful strategy of building new types of metal phosphonate hybrids is to introduce a second organic ligand such as oxalate, carboxylic acid, 2,2'-bipyridine, 4,4'-bipyridine, or 1,10-phenanthroline into the structures of metal phosphonates.⁵ Results from ours and other groups indicate that the introduction of a second organic ligand has been proved to be an effective synthetic method in the synthesis of metal phosphonates with new structure types and interesting properties. Recently, a series of novel metal phosphonate hybrids with mixed ligands have also been obtained by our group.⁶ The use of additional bidentate metal linkers such as 2,2'-bipy, 4, 4'-bipy, and 1,10-phen has been successful for building mixed-metal hybrid structures of V and Mo as well as other transition metal hybrid compounds with chain, layered, and 3D network structures.⁷ In recent articles, our group introduced the use of 2,2'-bipy or 1,10-phen as a decorating ligand in addition to the diphosphonate bridging ligand.⁸ In this context, very important is the role played by some non-covalent intermolecular forces, as the π - π stackings and the hydrogen bonding interactions to increase the dimensionality of the polymerization. In this work, by employing 4-carboxyphenylphosphonic acid (4-cppH₃) as the phosphonate ligand and 2,2'-bipy, 4,4'-bipy or 1,10-phen as the second metal linker, we have successfully obtained four novel cadmium carboxyphosphonates with 2D layered and 3D supramolecular structure, namely, Cd₃[(4-cppH)₂(4-cppH₂)₂] (**1**), Cd[(2,2'-bipy)(4-cppH)] (**2**), [Cd₃(1,10-phen)₃(4-cpp)₂] \cdot 6H₂O (**3**) and [Cd(4,4'-bipy)(4-cppH)(H₂O)₂] \cdot 2H₂O (**4**). Herein, we report their syntheses, crystal structures, thermal stabilities, and luminescence properties. The molecular recognition property of compound **1** has also been studied. At present, research on the properties of metal phosphonates is mainly focused on the magnetism, luminescence, proton conductivity and ion exchange etc. To the best of our knowledge, no metal phosphonate hybrids have been realized so far for their molecular recognition properties, this is the first example of the studies on molecular recognition property of metal phosphonates. Further work is in progress to synthesize metal phosphonate hybrids with molecular recognition property.

Experimental

Materials and measurements

The 4-carboxyphenylphosphonic acid (4-cppH₃) was synthesized according to published method.⁹ All chemicals were used as obtained without further purification. C, H and N content was determined by using a PE-2400 elemental analyzer. Cd and P content was determined by using an inductively coupled plasma (ICP) atomic absorption spectrometer. IR spectra were recorded on a Bruker AXS TENSOR-27 FT-IR spectrometer with KBr pellets in the range 4000–400 cm⁻¹. The X-ray powder diffraction data was collected on a Bruker AXS D8 Advance diffractometer using Cu-K α radiation ($\lambda = 1.5418 \text{ \AA}$) in the 2θ range of 5–60° with a step size of 0.02° and a scanning rate of 3°/min. Thermogravimetric (TG) analyses were performed on a Perkin–Elmer Pyris Diamond TG–DTA thermal analyses system in static air with a heating rate of 10 K min⁻¹ from 50 to 1000°C. The luminescence analyses were performed on a HITACHI F-7000 spectrofluorimeter. The luminescent properties of compounds **1–4** in the solid state, and compounds **1–4** in solvent emulsions were investigated at room temperature. The emulsions were prepared by introducing each sample (1.0 mg) as a powder into different solvents (each 4.0 ml). The luminescence spectra of the emulsions were measured after aging overnight.

Crystallographic studies

Data collections for compounds **1–4** were performed on the Bruker AXS Smart APEX II CCD X–diffractometer equipped with graphite monochromated MoK α radiation ($\lambda = 0.71073 \text{ \AA}$) at 293 \pm 2K. An empirical absorption correction was applied using the SADABS program. All structures were solved by direct methods and refined by full matrix least-squares fitting on F^2 by SHELXS-97.¹⁰ All non-hydrogen atoms were refined anisotropically. Hydrogen atoms except those for water molecules were generated geometrically with fixed isotropic thermal parameters and included in the structure factor calculations. Hydrogen atoms for water molecules were not included in the refinement. Details of crystallographic data of compounds **1–4** are summarized in Table 1. Hydrogen bonds for compounds **1** and **4** are given in Table 2. Selected bond lengths and angles of compounds **1–4** are listed in Table S1–S4 (ESI).

Synthesis of compounds 1–4

Cd₃[(4-cppH)₂(4-cppH₂)₂] (1). A mixture of Cd(Ac)₂·2H₂O (0.20 g, 0.75 mmol), 4-cppH₃ (0.10 g, 0.52 mmol) and H₂C₂O₄·2H₂O (0.06 g, 0.44 mmol) was dissolved in 8 mL distilled water. The resulting solution was stirred for about 1h at room temperature, sealed in a 20 mL Teflon-lined stainless steel autoclave, and heated at 180 °C for 3 days under autogenous pressure. After the mixture was cooled slowly to room temperature, the colorless block crystals of **1** were obtained. Yield: 58.2 % (based on Cd). Anal. Calc. for C₂₈H₂₂Cd₃O₂₀P₄: C, 29.51; H, 1.95; P, 10.87; Cd, 29.60. Found: C, 29.58; H, 1.91; P, 10.82; Cd, 29.65 %. IR (KBr, cm⁻¹): 3462(s), 2925(m), 2853(m), 1623(s), 1460(w), 1388(w), 1318(m), 1086(w), 1027(w), 982(w), 785(m), 709(w), 528(m).

Cd[(4-cppH)(2,2'-bipy)] (2). A mixture of Cd(Ac)₂·2H₂O (0.11 g, 0.43 mmol), 4-cppH₃ (0.05 g, 0.26 mmol) and 2,2'-bipy (0.07 g, 0.44 mmol) was dissolved in 10 mL distilled water. The resulting solution was stirred for about 1h at room temperature, sealed in a 20 mL Teflon-lined stainless steel autoclave, and heated at 80 °C for 5 days under autogenous pressure. After the mixture was cooled slowly to room temperature, the colorless block crystals of **2** were obtained. Yield: 68.4 % (based on Cd). Anal. Calc. for C₁₇H₁₇CdN₂O₇P: C, 40.46; H, 3.40; N, 5.55; P, 6.14; Cd, 22.27. Found: C, 40.50; H, 3.36; N, 5.51; P, 6.18; Cd, 22.32 %. IR (KBr, cm⁻¹): 3514(m), 1589(s), 1526(s), 1474(w), 1402(s), 1149(m), 1117(m), 1065(s), 1013(m), 916(s), 858(s), 736(s), 650(m), 598(m), 463(m).

[Cd₃(4-cpp)₂(1,10-phen)₃]·6H₂O (3). A mixture of Cd(Ac)₂·2H₂O (0.11 g, 0.43 mmol), 4-cppH₃ (0.05 g, 0.26 mmol) and 1,10-phen (0.09 g, 0.44 mmol) was dissolved in 10 mL distilled water. The pH value was adjusted to 5.5 by adding 1 M aqueous NaOH dropwise. The resulting solution was stirred for about 1h at room temperature, sealed in a 20 mL Teflon-lined stainless steel autoclave, and heated at 140 °C for 3 days under autogenous pressure. After the mixture was cooled slowly to room temperature, the colorless block crystals of **3** were obtained. Yield: 36.2 % (based on Cd). Anal. Calc. for C₅₀H₄₄Cd₃N₆O₁₆P₂: C, 43.39; H, 3.20; N, 6.07; P, 4.48; Cd, 24.36. Found: C, 43.35; H, 3.23; N, 6.03; P, 4.52; Cd, 24.31 %. IR (KBr, cm⁻¹): 3440(s), 1638(w), 1588(m), 1531(m), 1393(m), 1070(m), 965(m), 857(m), 780(w), 730(m), 598(w).

[Cd(4-cppH)(4,4'-bipy)(H₂O)₂]·2H₂O (4). A mixture of Cd(Ac)₂·2H₂O (0.11 g, 0.43 mmol), 4-cppH₃ (0.05 g, 0.26 mmol) and 4,4'-bipy (0.08 g, 0.44 mmol) was dissolved in 10 mL distilled water. The resulting solution was stirred for about 1h at room temperature, sealed in a 20 mL Teflon-lined stainless steel autoclave, and heated at 180 °C for 3 days under autogenous pressure. After the mixture was cooled slowly to room temperature, the colorless block crystals of **4** were

obtained. Yield: 72.3 % (based on Cd). Anal. Calc. for $C_{17}H_{21}CdN_2O_9P$: C, 37.76; H, 3.91; N, 5.18; P, 5.73; Cd, 20.79. Found: C, 37.72; H, 3.93; N, 5.15; P, 5.78; Cd, 20.73 %. IR (KBr, cm^{-1}): 3435(m), 3054(w), 2925 (m), 2583(w), 1596(s), 1537(m), 1388(m), 1211(w), 1117(m), 1052(m), 968(w), 806(w), 722(m), 632(w), 591(w), 508(w).

Results and discussion

Syntheses

By using the 4-cppH₃ as the phosphonate ligand, compounds **1–4** have been successfully synthesized under hydrothermal conditions. Product composition depends on a series of critical conditions, including pH of the medium, temperature, hence pressure, the presence of structure-directing cations, and the use of mineralizers. Compound **1** was received when the molar ratio of Cd²⁺, 4-cppH₃ and H₂C₂O₄·2H₂O is 8:6:5 at their original pH. H₂C₂O₄ molecular play an important role in the formation of compound **1**. We did not successfully obtain compound **1** without the presence of H₂C₂O₄ molecule. And compound **1** also could not be prepared when we replace it with HCl under the same pH value. Even if the H₂C₂O₄ were not included in the final product, its inclusion in the reactive mixture is crucial to isolate good-quality single crystals of compound **1**. Compounds **2–4** were all obtained with the molar ratio Cd²⁺/4-cppH₃/2,2'-bipy, 1,10-phen or 4,4'-bipy = 5: 3: 5. Despite our efforts to grow single-crystals of compounds **2–4** with other molar ratios, we were not successful in obtaining good samples for X-ray diffraction studies. The pH value was also very important for the formation of suitable single-crystals. It was found that pure phases of compounds **1**, **2** and **4** can be obtained with good yields and best crystallinity when the pH values are 4.0 for compounds **1**, **2** and 5.0 for compound **4**, respectively. Compound **3** with best crystal quality was obtained in the pH value of 5.0, but less gray powder was observed. The reaction mixture with a pH value of 5.5 yields the pure phase of the sample, while the pH value above 6 results in flocculent mixture without the formation of **3**. The powder XRD patterns and the simulated XRD patterns of the four title compounds are shown in supporting information (see Fig. S1–S4, ESI). The Powder X-ray diffraction patterns of compounds **1–4** all match those simulated from single-crystal X-ray data, clearly indicating that the pure phases are obtained.

Description of structure 1

Compound **1** crystallizes in a triclinic space group $P-1$ (see Table 1). The asymmetric unit contains three crystallographically unique Cd(II) ions, two 4-cppH^{2-} anions and two 4-cppH_2^- anions. All Cd(II) ions hold $\{\text{CdO}_6\}$ octahedral geometries (Fig. 1). Cd1 ion is six-coordinated by six phosphonate oxygen atoms (O2, O3, O5, O9, O10B, and O12A) from five carboxyphosphonate ligands. Cd2 ion is also six-coordinated by six phosphonate oxygen atoms (O2C, O3D, O6E, O7C, O8D, and O10) from six carboxyphosphonate ligands. Cd3 ion is still six-coordinated by six phosphonate oxygen atoms (O1, O5C, O6D, O7, O8, and O12) from five carboxyphosphonate ligands. The Cd–O bond lengths are in the range of 2.174(19) to 2.535(18) Å (Table S1, ESI), compared with those observed in the other Cd–O complexes with octahedral environment. All the lengths of Cd–O bonds are in normal range.¹¹

Scheme 1

Table 1

Fig. 1

In compound **1**, the phosphonate oxygen atoms of carboxyphosphonate ligand are all coordinated, but all the oxygen atoms of the carboxylate groups are not involved in the coordination of the metal ions. The carboxyphosphonate ligands adopt two different types of chelating and bridging modes, the 4-cppH^{2-} anion functions as a pentadentate ligand and links with four Cd(II) ions through three phosphonate oxygen atoms (Scheme 1a). The 4-cppH_2^- anion functions as a tetradentate metal linker, binding four Cd(II) ions through two phosphonate oxygen atoms (Scheme 1b). The phosphonate oxygen atoms (O2, O3, O7, O8) in 4-cppH^{2-} anions and oxygen atoms (O5, O6, O10, O12) in 4-cppH_2^- anions are all bidentately bridging, whereas the phosphonate oxygen atoms (O1 and O9) in 4-cppH^{2-} anions are unidentate. Based on the charge balance, the phosphonate oxygen atoms (O4, O11) in 4-cppH_2^- anions are protonated, and all the carboxylate oxygen atoms are protonated.

Fig. 2

Table 2

Fig. 3

The overall structure of compound **1** can be described as a 3D supramolecular network. As shown in Fig. 2a. $\{Cd(1)O_6\}$, $\{Cd(2)O_6\}$, and $\{Cd(3)O_6\}$ polyhedra are interconnected into a 1D chain along the *b*-axis *via* edge-sharing. Adjacent chains are further linked into a 2D layer in *ab* plane by the $\{CPO_3\}$ tetrahedra (Fig. 2b). The carboxylate moieties of the phosphonate ligand are orientated into the interlayer space. There are two kinds of hydrogen bonds between the carboxylate oxygen (O15) and (O19) with the distances of 2.71(2) Å (O15–H15A \cdots O19), between (O16) and (O20) with the distances of 2.60(2) Å (O20–H20A \cdots O16), respectively. The interactions contribute to form a 3D supramolecular network (see Fig. 3 and Table 2).

Description of structure 2

Compound **2** crystallizes in a monoclinic space group *C2/c* (see Table 1). The asymmetric unit contains one Cd(II) ion, one 4-cppH²⁻ anion and one 2,2'-bipy molecule (Fig. 4). Cd1 ion is six-coordinated to give a $\{CdO_4N_2\}$ octahedral geometry (Fig. 5). Two of the six coordination positions are filled with two phosphonate oxygen atoms (O1, O2A) from two 4-cppH²⁻ anions. The remaining sites are occupied by two carboxylate oxygen atoms (O4B, O5B) from one 4-cppH²⁻ anion and two nitrogen atoms (N1, N2) from one 2, 2'-bipy molecule. The Cd–O [2.179(2)–2.478(7) Å] and Cd–N [Cd(1)–N(1) = 2.349(2), Cd(1)–N(2) = 2.346(3) Å] distances are comparable to those in other reported cadmium(II) phosphonates (Table S2, ESI).¹² The carboxyphosphonate ligand serves as a tetradentate ligand, binding three Cd(II) ions through two phosphonate oxygen atoms (O1, O2) and two carboxylate oxygen atoms (O4, O5) (Scheme 1c). It chelates one Cd1 ion through two carboxylate oxygen atoms (O4, O5). The phosphonate oxygen atom (O3) of the 4-cppH²⁻ anion is 1H-protonated based on the requirement of charge balance.

Fig. 4

Fig. 5

Fig. 6

As shown in Fig. 5, compound **2** shows a layer structure. The $\{Cd(1)O_4N_2\}$ polyhedra and $\{CPO_3\}$ tetrahedra are interconnected into a tetranuclear cluster *via* corner-sharing. Such neighboring tetranuclear clusters are further connected to form a 2D layer through carboxyphosphonate ligands in *ab* plane, and 2, 2'-bipy molecules hung up in these layers (Fig. 6).

Description of structure 3

X-ray single crystal diffraction revealed that compound **3** crystallizes in a triclinic space group $P-1$ (see Table 1). The asymmetric unit contains three Cd(II) ions, two 4-cpp³⁻ anions, three 1,10-phen molecules and six lattice water molecules (Fig. 7). Cd1 ion is six-coordinated by four phosphonate oxygen atoms (O1, O2, O3A and O4) from three separate 4-cpp³⁻ anions and two nitrogen atoms (N1, N2) from one 1,10-phen molecule. Cd2 ion also adopts a six-coordinated state by one phosphonate oxygen atom (O5) from one 4-cpp³⁻ anion, three carboxylate oxygen atoms (O7B, O8B, and O9C) from two 4-cpp³⁻ anions and two nitrogen atoms (N3, N4) from one 1,10-phen molecule. Cd3 ion is five-coordinated by three phosphonate oxygen atoms (O1, O2A, and O6A) from three 4-cpp³⁻ anions and two nitrogen atoms (N5, N6) from one 1,10-phen molecule. The bond lengths of Cd–O and Cd–N are in the range of 2.155(5)–2.524(5) Å and 2.308(6)–2.384(6) Å respectively (Table S3, ESI), which are comparable to those reported for other cadmium(II) phosphonates.^{11, 12} In compound **3**, the two 4-cpp³⁻ ligands display two different kinds of coordination modes. The coordination mode of the first 4-cpp³⁻ anion can be described as a hexadentate bridging mode. It links five Cd(II) ions through its three phosphonate oxygen atoms (O1, O2 and O3) and one carboxylate oxygen atom (O9) (Scheme 1d). The phosphonate oxygen atoms (O1, O2) are both bidentately bridging, where as the remaining phosphonate oxygen atom (O3) is unidentate. The second 4-cpp³⁻ ligand acts as a pentadentate ligand, binding four Cd(II) ions through all its phosphonate oxygen atoms and carboxylate oxygen atoms (Scheme 1e). It chelates one Cd2 ion through two carboxylate oxygen atoms (O7, O8). The three phosphonate oxygen atoms (O4, O5 and O6) are all unidentate.

Fig. 7

Fig. 8

Fig. 9

The overall structure of compound **3** can be described as a 3D supramolecular structure. The two {Cd(2)O₄N₂} polyhedra and two {CPO₃} tetrahedra are interconnected into one unit by bridging and chelating 4-cpp³⁻ anions, two {Cd(1)O₄N₂} polyhedra, two {Cd(3)O₃N₂} polyhedra and two {CPO₃} tetrahedra are linked into another unit *via* corner-sharing. The interconnection of such units are connected into a 1D chain along the *a*-axis *via* corner-sharing, and these chains are

interconnected by carboxyphosphonate ligands to form a 2D inorganic layer in *ac* plane. As shown in Fig. 8, there are two distinct types of window systems running along *b*-axis. The window (A) is assembled with 36 atoms [$16.7 \text{ \AA} (P1-P2) \times 5.7 \text{ \AA} (C3-C9)$], while the window (B) is assembled with 26 atoms [$10.2 \text{ \AA} (O5-O5) \times 6.6 \text{ \AA} (C14-C14)$]. Interestingly the windows arranged in an alternative sequence (ABAB). Then the adjacent layers are further assembled into a 3D supramolecular structure through π - π stacking interactions (Fig. 9). The π - π stacking interactions can play an important role in controlling the packing or assembly of compounds. The usual π interaction is an offset or slipped stacking of the aromatic nitrogen heterocycles or benzene rings. In the two interactions, the effective distance is in the range of 3.3 to 3.8 \AA . In compound **3**, the 1,10-phen rings between the neighboring asymmetric unit are parallel to each other, and the face-to-face distance (3.53 \AA and 3.73 \AA) between adjacent 1,10-phen rings is in the normal range for such interactions, hence there are π - π stacking interactions.

Description of structure 4

Compound **4** crystallizes in a monoclinic space group $P2(1)/c$ (see Table 1). The asymmetric unit of compound **4** is shown in Fig. 10. It contains one Cd(II) ion, one 4-cppH²⁻ anion, one 4,4'-bipy molecule, two coordinated water molecules, and two lattice water molecules. Cd1 ion exhibits a six-coordinated environment. The six coordination positions are filled with two phosphonate oxygen atoms (O1, O2A) from two 4-cppH²⁻ anions, two nitrogen atoms (N1, N2B) from two 4,4'-bipy molecules and two oxygen atoms (O6, O7) from two coordinated water molecules. The bond lengths of Cd–O and Cd–N are in the range of 2.225(3)–2.435(4) \AA and 2.364(4)–2.367(4) \AA , respectively. These values are in agreement with those reported for other cadmium(II) phosphonate compounds (Table S4, ESI).¹³ The 4-cppH²⁻ anion is a bidentate ligand, binding two separate Cd1 ions through two phosphonate oxygen atoms (O1, O2), respectively (Scheme 1f).

Fig. 10

Fig. 11

Fig. 12

The $\{\text{Cd}(1)\text{O}_4\text{N}_2\}$ polyhedra and $\{\text{CPO}_3\}$ tetrahedra are interconnected into a 1D chain along the *b*-axis *via* corner-sharing (Fig. 11a). Adjacent so-built chains are further linked into a 2D layer in

ab plane by the 4,4'-bipy molecules, with 4-cppH²⁻ groups hung up in these layers (Fig. 11). The lattice water molecules are located at the neighbor layers, as shown in Fig. 12, these neighboring layers interdigitate through hydrogen bonding interactions to give rise to a 3D supramolecular network structure. The O...O distances are 2.724(5), 2.720(5), 2.786(5), 2.712(5), 2.847(6) and 2.548(5) Å for O(1W)–H(1WB)...O(4), O(7)–H(7B)...O(1W), O(1W)–H(1WA)...O(6), O(2W)–H(2WA)...O(3), O(2W)–H(2WC)...O(3) and O(5)–H(5A)...O(2W), respectively. (see Fig. 12a and Table 2).

IR spectra

The IR spectra for compounds **1–4** are recorded in the region 4000–400 cm⁻¹ (Fig. S5–S8, ESI). The absorption bands at 3462 cm⁻¹ for **1**, 3514 cm⁻¹ for **2**, 3440 cm⁻¹ for **3**, and 3435 cm⁻¹ for **4** can be assigned to the O–H stretching vibrations.^{14a} The broad bands at 1638, 1393 cm⁻¹ for **1**, 1596, 1388 cm⁻¹ for **4** are assigned to the C=O asymmetric and symmetric stretching vibration of the carboxylic acid group. These rather low positions are due to the strong hydrogen bonds.^{14b} While the bands at 1589, 1526, 1474, 1402 cm⁻¹ for compound **2**, 1638, 1588, 1531, 1393 cm⁻¹ for compound **3**, which are assigned to the antisymmetrical and symmetrical stretching vibrations of C–O bonds of the carboxylate groups. It is attributed to the carboxylate groups coordinated to the metal. Thus the carboxylate groups are deprotonated and in agreement with structural results. The bands at 1589, 1526, 1402 cm⁻¹ for **2** can be assigned to the stretching bands of the pyridyl rings of 2,2'-bipy ligands. The bands at 1588, 1531, 1393 cm⁻¹ for **3** can be assigned to the stretching bands of the 1,10-phenanthroline ligands. While the bands at 1596, 1537, 1388 cm⁻¹ for **4** can be assigned to the stretching bands of the 4,4'-bipy ligands.¹⁵ Strong bands between 1200 and 900 cm⁻¹ for four compounds are due to stretching vibrations of the tetrahedral {CPO₃} groups, as expected.¹⁶

Thermal analysis

In order to examine the thermal stabilities of compounds **1–4**, thermogravimetric analyses were performed in static air atmosphere. The TG curve shows one step of weight loss for compound **1**, which is stable up to a high temperature of 338 °C (Fig. S9 and Fig. S13, ESI). Compared with the other metal phosphonates reported by our group, the high thermal stability phenomenon is unusual.^{8a, 8b} The weight loss between 338 °C and 509 °C, the observed weight loss is 36.0 %, corresponding to the pyrolysis of the organic moieties. The final product of the thermal process is

CdO on the basis of powder X-ray diffraction (Fig. S14, ESI), and P_2O_5 is lost as gas. The total weight loss of 39.4 % is smaller than the calculated value (41.3 %). The TGA curve of compound **2** reveals two main steps of weight loss (Fig. S10, ESI). The first step started at 50 °C and completed at 120 °C, corresponding to elimination of the organic moieties and the collapse of the structures. The second step weight loss covers a temperature range from 244 to 658 °C, which corresponds to the further decomposition of the compound. The total weight loss is 60.5 %. Above 850 °C, the further decomposition of the organic groups results in an amorphous phase that was not characterized. The compound **3** also indicates two main steps of weight loss (Fig. S11, ESI). The first step between 50 and 120 °C corresponds to the release of six lattice water molecules. The weight loss of 6.8 % is close to the calculated value (7.8 %). The second step from 252 to 805 °C, which corresponds to the combustion of organic groups. The total weight loss is 63.6 %. We try to confirm the supposition by PXRD, but the final residues are unidentified because they are amorphous. The TGA curve of compound **4** still shows two steps (Fig. S12, ESI). The weight loss between 50 and 130 °C corresponds to the release of two lattice water molecules and two coordinated water molecules. The weight loss of 11.8 % is close to the calculated value (13.3 %). Between 165 and 518 °C, there is a complicated weight loss, corresponding to elimination of the organic moieties and the collapse of the structures. The total weight loss is 61.1 %. The product of the thermal decomposition is amorphous and was not further characterized.

Luminescent properties

The solid-state emission spectra of free 4-cppH₃, the second ligands (see Fig. S15–S17, ESI) and compounds **1–4** were measured at room temperature. As show in Fig. 13a, the free carboxyphosphonate ligand 4-cppH₃ exhibits an emission band at 356 nm upon excitation at 318 nm. Compared to the free ligand, under the same experimental conditions compound **1** gives a fluorescent emission at $\lambda_{\max} = 355$ nm upon complexation of the 4-cpp³⁻ ligands with the Cd^{II} ions. The emission may be assigned to the ligand-centered $\pi-\pi^*$ transition because their fluorescent emission bands are very similar to that of the free ligand.¹⁷ Compound **1** shows obviously weakened intensity. It is proved that metal ions in the structures may change intraligand transitions.¹⁸ Compound **2** displays a luminescent emission band at $\lambda_{\max} = 357$ nm upon complexation of both 4-cpp³⁻ and 2,2'-bipy ligands with the Cd(II) ions. This emission can also be assigned to the intraligand transition.

Fig. 13

Compounds **3** and **4** exhibit blue fluorescent emission bands at 374 nm and 414 nm, respectively (Fig. 13). It is clear that compounds **3** and **4** show red-shifted emission band to different extents with slightly weakened intensities compared with the free 4-cppH₃ ligand, which is probably originated from the ligand-to-metal charge transfer (LMCT).¹⁹ Under the same measurement conditions, the luminescent behaviors of compounds **1–4** are distinctly different. By introduction of the second metal linker, the intensities of emission band have been obviously weakened for compounds **2–4** and significant red shift for compounds **3** and **4**. The differences indicate that the position and intensity of emission band can be changed by second ligands. This phenomenon shows that the luminescence behavior is closely associated with the ligands coordinated around the center Cd(II) ions. Luminescent properties of compounds **1–4** indicate that they are good candidates for blue–light luminescent materials.

Molecular Recognition Properties

The molecular recognition, an important process in biological and chemical systems, has been used to investigate straightforward and highly sensitive sensing of small molecules.²⁰ The differential recognition/binding events with guest molecules confined by the tunable pore sizes and functionalized pore surfaces, which can be transduced into externally optical signals, have enabled the MOFs to become a new type of sensing materials.²¹ The fluorescence properties of compounds **1–4** in different solvent emulsions were investigated for the sensing of small molecules. The emulsions were prepared by introducing 1.00 mg of compounds **1–4** powders into 4.00 mL of alkyl alcohol and carbonyl derivatives, such as acetone, 1-propanol, 1-pentanol, methanol, 1-butanol, ethanol, DMF, N,N-Dimethylacetamide, cyclohexanone and 4-methyl-2-pentanone at room temperature.

Fig. 14

Fig. 15

For compounds **2–4**, they did not exhibit the potential for the sensing of guest molecules (Fig. S18–S20, ESI). While under similar measurement conditions, the fluorescence property indicates that the solvent molecules play an important role in compound **1**, particularly in the case of DMF and acetone, which exhibit the most significant enhancing and quenching effects, respectively (Fig. 14). For further exploration, we examined the molecular recognition properties of compound **1** in detail. Compound **1** was dispersed in 1-propanol as the standard emulsion, while the solvent content was gradually increased to monitor the emissive response. As shown in Fig. 15a, the fluorescence intensity of compound **1** gradually increased with the addition of DMF solvent. While the content of acetone solvent in the emulsion of compound **1** was improved, the fluorescence intensity was evidence quenched (Fig. 15b). And the fluorescence properties of compound **1** emulsion did not exhibit regular variation in the presence of various contents of methanol, ethanol, 1-butanol, 1-pentanol, N,N-Dimethylacetamide, cyclohexanone and 4-methyl-2-pentanone (Fig. S21–S27, ESI). It is interesting that the structures of DMF, acetone, N,N-Dimethylacetamide, cyclohexanone and 4-methyl-2-pentanone all contain –CO– functional groups. Then we compared the sensing of these carbonyl derivatives in detail. There exist responses of compound **1** to N,N-Dimethylacetamide, cyclohexanone and 4-methyl-2-pentanone, but regular response of luminescent intensity fails to appear with the increase on concentration. Herein, the changes of luminescent intensity on compound **1** were just particular and regular by improving the content of DMF and acetone. It is further indicated that compound **1** showed a selective sieving function to DMF and acetone solvents.

This phenomenon may be attributed to the difference in structures of compounds **1–4**. The most significant structural feature of compound **1** is the presence of supramolecular network structure within the uncoordinated carboxylate oxygen atoms, highlighting the potential for its recognition of small molecules. We surmise that the uncoordinated carboxylate oxygen atoms might enhance the interaction between compound **1** and the guest molecules. The detailed mechanism is under investigation. In the structures of compounds **2** and **3** all carboxylate oxygen atoms are coordinated, so the interactions between the compounds and guest molecules are inexistent. In compound **4**, the uncoordinated carboxylate oxygen atoms are also observed, but the steric barrier in structure lead to the failure of molecular recognition. Thus, only compound **1** can be a good material used for the sensing of guest molecules. To check the structural transformation, the PXRD measurement of compound **1** into DMF solvent after aging has also been done. The powder X-ray diffraction shows

obviously weakened intensity than the original one. In our opinion, this phenomenon is due to the interaction of compound **1** with the solvent molecule (Fig. S28, ESI). Therefore, this highly sensing function of compound **1** indicates the promise of this type of luminescent materials for the sensing of substrates in biological systems.²²

Conclusion

In this paper, four new cadmium carboxyphosphonates with 2D layered and 3D supramolecular structure, namely, $\text{Cd}_3[(4\text{-cppH})_2(4\text{-cppH}_2)_2]$ (**1**), $\text{Cd}[(2,2'\text{-bipy})(4\text{-cppH})]$ (**2**), $[\text{Cd}_3(1,10\text{-phen})_3(4\text{-cpp})_2]\cdot 6\text{H}_2\text{O}$ (**3**) and $[\text{Cd}(4,4'\text{-bipy})(4\text{-cppH})(\text{H}_2\text{O})_2]\cdot 2\text{H}_2\text{O}$ (**4**), have been synthesized under hydrothermal conditions. In compound **1**, $\{\text{Cd}(1)\text{O}_6\}$, $\{\text{Cd}(2)\text{O}_6\}$, $\{\text{Cd}(3)\text{O}_6\}$ and $\{\text{CPO}_3\}$ polyhedra form a layer in *ab* plane *via* edge- and corner-sharing. Neighboring layers compose into a 3D supramolecular network by hydrogen bonding interactions. The structure of compound **2** shows a novel layered structure, in which the interconnection of two $\{\text{Cd}(1)\text{O}_4\text{N}_2\}$ and two $\{\text{CPO}_3\}$ polyhedra *via* corner-sharing forms a tetranuclear cluster, the so-built tetranuclear clusters are bridged by the phosphonate ligands into a 2D layer. For compound **3**, $\{\text{Cd}(1)\text{O}_4\text{N}_2\}$, $\{\text{Cd}(2)\text{O}_4\text{N}_2\}$, $\{\text{Cd}(3)\text{O}_3\text{N}_2\}$ and $\{\text{CPO}_3\}$ polyhedra are interconnected by carboxyphosphonate ligands to a 2D layer in *ac* plane. Then the adjacent layers are further assembled into a 3D supramolecular structure through π - π stacking interactions. In compound **4**, $\{\text{CdO}_4\text{N}_2\}$ polyhedra and $\{\text{CPO}_3\}$ tetrahedra are linked by 4,4'-bipy molecules into a 2D layer, which are further assembled into a 3D supramolecular structure *via* the hydrogen-bonding interactions. The luminescent properties of compounds **1-4** indicate that they are good candidates for blue-light luminescent materials, and compound **1** may be potentially used for the sensing of DMF and acetone.

Acknowledgments

This work is supported by the National Natural Science Foundation of China (Grant No. 21371085).

Electronic supplementary information (ESI) available: XRD patterns, IR spectra and thermal analyses for compounds **1-4**. The PXRD patterns for compound **1** on heating from 25 to

350 °C. XRD patterns of the final products in the thermal decomposition for compound **1**. The solid-state luminescent properties of 2,2'-bipy, 1,10-phen and 4,4'-bipy. The emission spectra of compounds **2–4** introduces into various pure solvents. The fluorescence properties of compound **1** emulsion in the presence of various contents of methanol, ethanol, 1-butanol, 1-pentanol, N,N-Dimethylacetamide, cyclohexanone and 4-methyl-2-pentanone. The PXRD patterns for compound **1** into DMF solvent after aging. Tables list selected bond lengths and bond angles for compounds **1–4** presented in this paper. CCDC 948271–948274 contain the supplementary crystallographic data for this paper. These data can be obtained free of charge www.ccdc.cam.ac.uk/conts/retrieving.html (or from the Cambridge Crystallographic Data Center, 12, Union Road, Cambridge CB21EZ, UK; fax: (+44) 1223-336-033; e-mail: deposit@ccdc.cam.ac.uk).

Notes and References

- (a) A. Clearfield and K. Demadis, *Metal Phosphonate Chemistry: From Synthesis to Applications*, Published by the Royal Society of Chemistry, Oxford, 2012, 164; (b) D. E. Katsoulis, *Chem. Rev.* 1998, **98**, 359; (c) J. T. Rhule, C. L. Hill and D. A. Judd, *Chem. Rev.* 1998, **98**, 327; (d) M. A. AlDamen, J. M. Clemente-Juan, E. Coronado, C. Martí-Gastaldo and ño Gaita-Ari, *A. J. Am. Chem. Soc.*, 2008, **130**, 8874; (e) T. Yamase, *Chem. Rev.* 1998, **98**, 307.
- (a) Z. X. Chen, Y. M. Zhou, L. H. Weng and D. Y. Zhao, *Cryst. Growth Des.*, 2008, **8**, 4045; (b) B. K. Tripuramallu, S. Mukherjee and S. K. Das, *Cryst. Growth Des.*, 2012, **12**, 5579; (c) W. T. Yang; H. Y. Wu, R. X. Wang, Q. J. Pan, Z. M. Sun and H. J. Zhang, *Inorg. Chem.*, 2012, **51**, 11458.
- (a) J. Weber, G. Grossmann, K.-D. Demadis, N. Daskalakis, E. Brendler, M. Mangstl and J.-S. Günne, *Inorg. Chem.*, 2012, **51**, 11466; (b) R. B. Fu, S. M. Hu and X. T. Wu, *CrystEngComm.*, 2013, **15**, 802; (c) P. O. Adelani and T. E. Albrecht-Schmitt, *Cryst. Growth Des.*, 2011, **11**, 4676.
- (a) W. Chu, Y. Y. Zhu, Z. G. Sun, C. Q. Jiao, J. Li, S. H. Sun, H. Tian and M. J. Zheng, *RSC Advances.*, 2013, **3**, 623; (b) D. P. Dong, Z. G. Sun, F. Tong, Y. Y. Zhu, K. Chen, C. Q. Jiao, C. L. Wang, C. Li and W. N. Wang, *CrystEngComm.*, 2011, **13**, 3317; (c) D. P. Dong, L. Liu, Z. G. Sun, C. Q. Jiao, Z. M. Liu, C. Li, Y. Y. Zhu, K. Chen and C. L. Wang, *Cryst. Growth Des.*, 2011,

- 11**, 5346; (d) N. Zhang, Z. G. Sun, Y. Y. Zhu, J. Zhang, L. Liu, C.-Y. Huang, X. Lu, W. N. Wang and F. Tong, *New J. Chem.*, 2010, **34**, 2429.
5. (a) P. F. Wang, Y. Duan, D. K. Cao, Y. Z. Li and L. M. Zheng, *Dalton Trans.*, 2010, **39**, 4559; (b) H. Y. Wu, W. T. Yang and Z. M. Sun, *Cryst. Growth Des.*, 2012, **12**, 4669; (c) Z. Y. Du, H. B. Xu, X. L. Li and J. G. Mao, *Eur. J. Inorg. Chem.*, 2007, 4520; (d) S. F. Tang, X. B. Pan, X. X. Lv, S. H. Yan, X. R. Xu, L. J. Li and X. B. Zhao, *CrystEngComm.*, 2013, **15**, 1860.
6. (a) K. Chen, Z. G. Sun, Y. Y. Zhu, Z. M. Liu, F. Tong, D. P. Dong, J. Li, C. Q. Jiao, C. Li and C. L. Wang, *Cryst. Growth Des.*, 2011, **11**, 4623; (b) L. Liu, Z. G. Sun, N. Zhang, Y. Y. Zhu, Y. Zhao, X. Lu, F. Tong, W. N. Wang and C. Y. Huang, *Cryst. Growth Des.*, 2010, **10**, 406; (c) Y. Zhao, C. Q. Jiao, Z. G. Sun, Y. Y. Zhu, K. Chen, C. L. Wang, C. Li, M. J. Zheng, H. Tian, S. H. Sun and W. Chu, *Cryst. Growth Des.*, 2012, **12**, 3191; (d) F. Tong, Z. G. Sun, K. Chen, Y. Y. Zhu, W. N. Wang, C. Q. Jiao, C. L. Wang and C. Li, *Dalton Trans.*, 2011, **40**, 5059; (e) Y. Y. Zhu, Z. G. Sun, F. Tong, Z. M. Liu, C. Y. Huang, W. N. Wang, C. Q. Jiao, C. L. Wang, C. Li and K. Chen, *Dalton Trans.*, 2011, **40**, 5584.
7. (a) Z. X. Chen, L. H. Weng and D. Y. Zhao, *Inorg. Chem. Commun.*, 2007, **10**, 447; (b) Y. Q. Guo, B. P. Yang, J. L. Song and J. G. Mao, *Cryst. Growth Des.*, 2008, **8**, 600; (c) J. T. Li, D. K. Cao, B. Liu, Y. Z. Li and L. M. Zheng, *Cryst. Growth Des.*, 2008, **8**, 2950.
8. (a) S. H. Sun, Z. G. Sun, Y. Y. Zhu, D. P. Dong, C. Q. Jiao, J. Zhu, J. Li, W. Chu, H. Tian, M. J. Zheng, W. Y. Shao and Y. F. Lu, *Cryst. Growth Des.*, 2013, **13**, 226; (b) M. J. Zheng, Y. Y. Zhu, Z. G. Sun, J. Zhu, C. Q. Jiao, W. Chu, S.-H. Sun and H. Tian, *CrystEngComm.*, 2013, **15**, 1445; (c) W. N. Wang, Z. G. Sun, Y. Y. Zhu, D. P. Dong, J. Li, F. Tong, C. Y. Huang, K. Chen, C. Li, C. Q. Jiao and C. L. Wang, *CrystEngComm.*, 2011, **13**, 6099.
9. (a) I. P. Beletskaya and M. A. Kazankova, *Russ. J. Org. Chem.*, 2002, **38**, 1391; (b) B. F. Hoskins, R. Robson and D. A. Slizys, *J. Am. Chem. Soc.*, 1997, **119**, 2952.
10. G.-M. Sheldrick, *SHELXS-97, Program for X-ray Crystal Structure Solution and Refinement*, University of Göttingen, Germany, 1997.
11. C. Y. Fang, Z. X. Chen, X. F. Liu, Y. T. Yang, M. L. Deng, L. H. Weng, Y. Jia and Y. M. Zhou, *Inorg. Chim. Acta.*, 2009, **362**, 2103.
12. Z. Y. Du, Y. H. Sun, S. Y. Zhang, Z. G. Zhou and Y. R. Xie, *J. Mol. Struct.*, 2010, **979**, 201.
13. J. Yang, J. F. Ma, G. L. Zheng, L. Li, F. F. Li, Y. M. Zhang and J. F. Liu, *Solid State Chem.*, 2003, **174**, 118.

14. (a) K. R. Ma, J. N. Xu, L. R. Zhang, J. Shi, D. J. Zhang, Y. L. Zhu, Y. Fan and T. Y. Song, *New J. Chem.*, 2009, **33**, 886; (b) S. Bauer, T. Bein and N. Stock, *Inorg. Chem.*, 2005, **44**, 5882.
15. (a) N. G. Armatas, W. Ouellette, K. Whitenack, J. Pelcher, H. X. Liu, E. Romaine, C. J. O'Connor and J. Zubieta, *Inorg. Chem.*, 2009, **48**, 8897; (b) R. T. Clarke, K. Latham, C. J. Rix and M. Hobday, *Chem. Mater.*, 2004, **16**, 2463.
16. (a) A. Cabeza, X. Ouyang, C. V. K. Sharma, M. A. G. Aranda, S. Bruque and A. Clearfield, *Inorg. Chem.*, 2002, **41**, 2325; (b) Z. M. Sun, J. G. Mao, B. P. Yang and S. M. Ying, *Solid State Sci.*, 2004, **6**, 295.
17. (a) J. Wu, H. W. Hou, H. Y. Han and Y. Fan, *Inorg. Chem.*, 2007, **46**, 7960; (b) Z. Z. Lai, R. B. Fu, S. M. Hu and X. T. Wu, *Eur. J. Inorg. Chem.*, 2007, **34**, 5439; (c) J. L. Song, H. H. Zhao, J. G. Mao and K. R. Dunbar, *Chem. Mater.*, 2004, **16**, 1884.
18. Y. Gong, W. Tang, W. B. Hou, Z. Y. Zha and C. W. Hu, *Inorg. Chem.*, 2006, **45**, 4987.
19. (a) J. Li, C. C. Ji, L. F. Huang, Y. Z. Li and H. G. Zheng, *Inorg. Chim. Acta.*, 2011, **371**, 33; (b) X. Q. Liu, Y. Y. Liu, Y. J. Hao, X. J. Yang and B. Wu, *Inorg. Chem. Commun.*, 2010, **13**, 513.
20. (a) T. M. Reineke, M. Eddaoudi, M. Fehr, D. Kelley and O. M. Yaghi, *J. Am. Chem. Soc.*, 1999, **121**, 1651; (b) O. M. Yaghi, G. Li and H. Li, *Nature.*, 1995, **378**, 703; (c) H. Li, M. Eddaoudi, T. L. Groy and O. M. Yaghi, *J. Am. Chem. Soc.*, 1998, **120**, 8571.
21. (a) Z. Y. Guo, H. Xu, S. Q. Su, J. F. Cai, S. Dang, S. C. Xiang, G. D. Qian, H. J. Zhang, M. O'Keeffe and B. L. Chen, *Chem. Commun.*, 2011, **47**, 5551; (b) Y. A. Li, S. K. Ren, Q. K. Liu, J. P. Ma, X. Y. Chen, H. M. Zhu and Y. B. Dong, *Inorg. Chem.*, 2012, **51**, 9629.
22. (a) B. L. Chen, Y. Yang, F. Zapata, G. N. Lin, G. D. Qian and E. B. Lobkovsky, *Adv. Mater.*, 2007, **19**, 1694; (b) H. Xu, F. Liu, Y. J. Cui, B. L. Chen and G. D. Qian, *Chem. Commun.*, 2011, **47**, 3153; (c) Y. J. Cui, Y. F. Yue, G. D. Qian and B. L. Chen, *Chem. Rev.*, 2012, **112**, 1126.

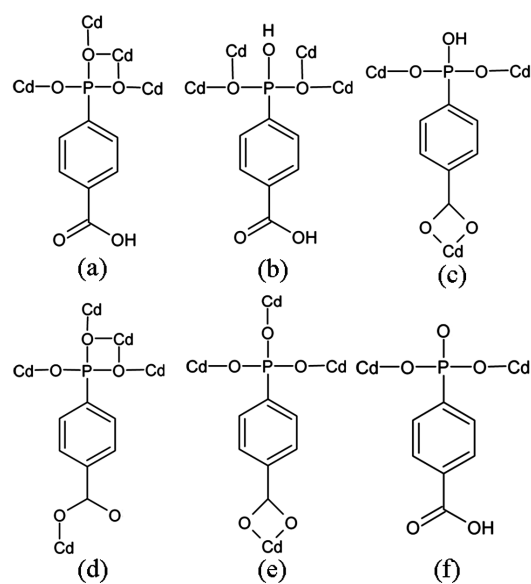
Table 1 Crystal data and structure refinement for compounds 1–4.

Compounds	1	2	3	4
Chemical formula	C ₂₈ H ₂₂ Cd ₃ O ₂₀ P ₄	C ₁₇ H ₁₇ CdN ₂ O ₇ P	C ₅₀ H ₄₄ Cd ₃ N ₆ O ₁₆ P ₂	C ₁₇ H ₂₁ CdN ₂ O ₉ P
Formula weight	1139.54	504.70	1384.05	540.73
Crystal system	Triclinic	Monoclinic	Triclinic	Monoclinic
Space group	<i>P</i> -1	<i>C</i> 2/ <i>c</i>	<i>P</i> -1	<i>P</i> 2(1)/ <i>c</i>
<i>a</i> / Å	5.6590(13)	18.2285(13)	13.9812(14)	11.7800(11)
<i>b</i> / Å	7.9562(18)	12.4643(9)	14.7218(14)	9.4034(9)
<i>c</i> / Å	19.147(4)	18.4247(19)	15.0185(14)	18.8322(18)
α (°)	96.620(3)	90	103.264(2)	90
β (°)	95.808(4)	117.2610(10)	92.471(2)	103.465(2)
γ (°)	98.313(3)	90	110.8650(10)	90
<i>V</i> (Å ³)	841.2(3)	3721.2(5)	2784.9(5)	2028.7(3)
<i>Z</i>	1	8	2	4
<i>D</i> _c / g·cm ⁻³	2.249	1.802	1.651	1.770
μ /mm ⁻¹	2.159	1.303	1.264	1.209
GOF on <i>F</i> ²	1.073	1.024	1.038	1.032
<i>R</i> , <i>R</i> _w [<i>I</i> >2 σ (<i>I</i>)]	0.0525, 0.1493	0.0264, 0.0613	0.0512, 0.1532	0.0415, 0.1053
<i>R</i> , <i>R</i> _w [all data]	0.0563, 0.1553	0.0396, 0.0701	0.0827, 0.1738	0.0653, 0.1166

$R_1 = \Sigma (|F_0| - |F_c|) / \Sigma |F_0|$, $wR_2 = [\Sigma w (|F_0| - |F_c|)^2 / \Sigma w F_0^2]^{1/2}$.

Table 2 Hydrogen bond distances (Å) and angles (°) for compounds **1** and **4**.

Compound 1				
D–H...A	D(D–H)/ Å	d(H...A)/ Å	D–H...A/ °	d(D...A)/ Å
O15–H15A...O19	0.85	1.87	167.7	2.71(2)
O20–H20A...O16	0.85	1.79	159.4	2.60(2)
Compound 4				
D–H...A	D(D–H)/ Å	d(H...A)/ Å	D–H...A/ °	d(D...A)/ Å
O(1W)–H(1WB)...O(4)	0.85	1.95	150.9	2.724(5)
O(7)–H(7B)...O(1W)	0.85	2.00	142.7	2.720(5)
O(1W)–H(1WA)...O(6)	0.85	2.17	129.1	2.786(5)
O(2W)–H(2WA)...O(3)	0.85	1.89	163.4	2.712(5)
O(2W)–H(2WC)...O(3)	0.85	2.05	156.8	2.847(6)
O(5)–H(5A)...O(2W)	0.85	1.72	162.6	2.548(5)



Scheme 1 The coordination modes of phosphonate ligands in compound **1** (a) and (b), compound **2** (c), compound **3** (d) and (e), and compound **4** (f).

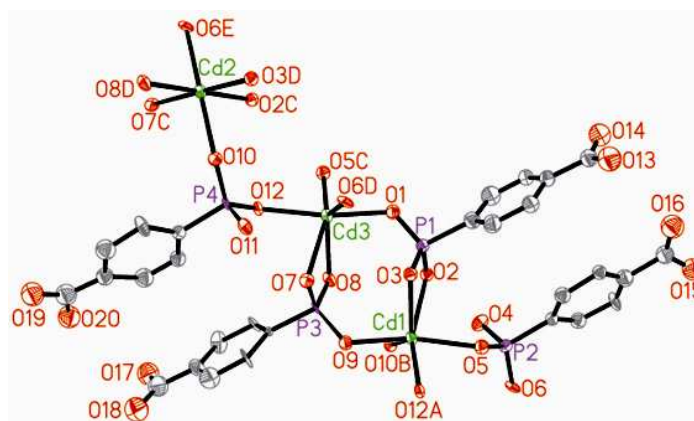


Fig. 1 Structure unit of compound **1** showing the atom labeling. Thermal ellipsoids are shown at the 50% probability level. All H atoms are omitted for clarity. Symmetry code for the generated atoms: A: $x, y - 1, z$; B: $x - 1, y - 1, z$; C: $x + 1, y + 1, z$; D: $x, y + 1, z$; E: $x + 1, y + 2, z$

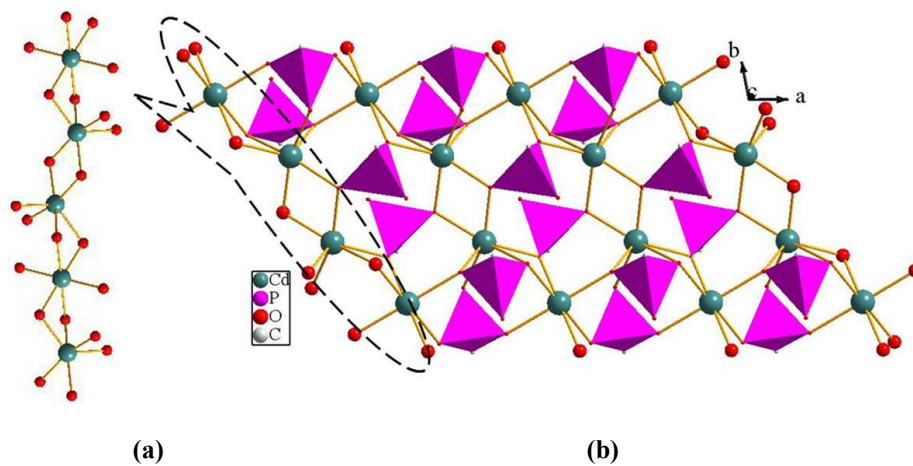


Fig. 2 (a) A 1D chain of {CdO₆} polyhedron along the *b*-axis; (b) The layer structure of compound **1** without the organic ligands viewed in *ab*-plane.

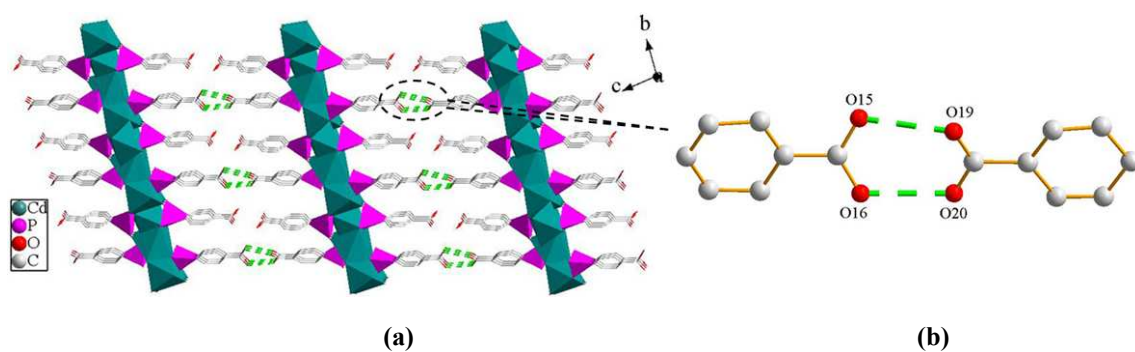


Fig. 3 (a) A polyhedral representation of the structure of compound **1** in the *bc*-plane. Green polyhedra: CdO₆, pink tetrahedra: CPO₃; (b) The connectivity of hydrogen bonds for compound **1**. All hydrogen atoms except for the hydrogen bonds are omitted for clarity.

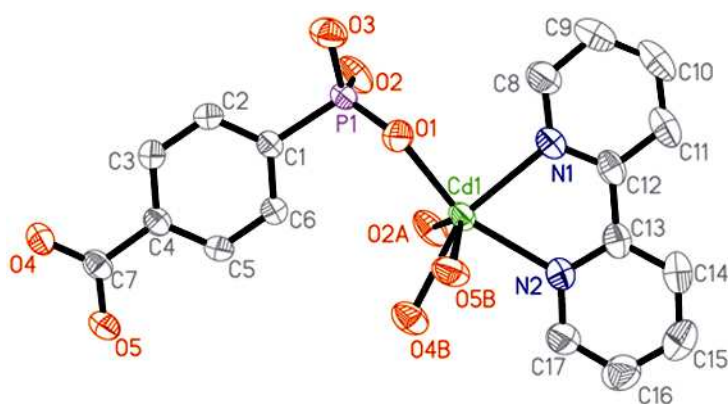


Fig. 4 Structure unit of compound **2** showing the atom labeling. Thermal ellipsoids are shown at the 50% probability level. All H atoms are omitted for clarity. Symmetry code for the generated atoms: A: $-x, -y + 2, -z$; B: $-x + 1/2, y - 1/2, -z + 1/2$.

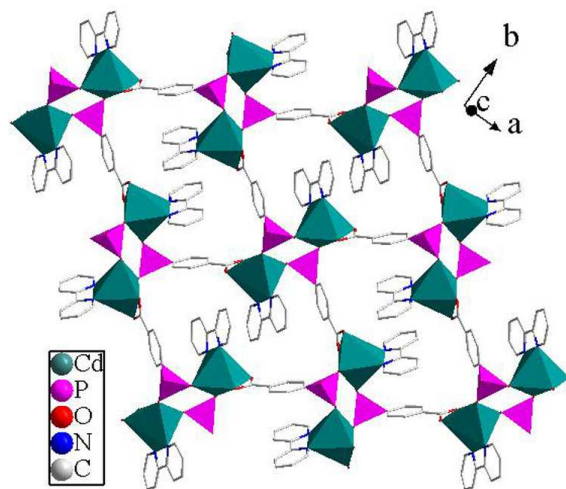


Fig. 5 The layer structure of compound **2** viewed in ab -plane. Green polyhedra: CdO_4N_2 , pink tetrahedra: CPO_3 .

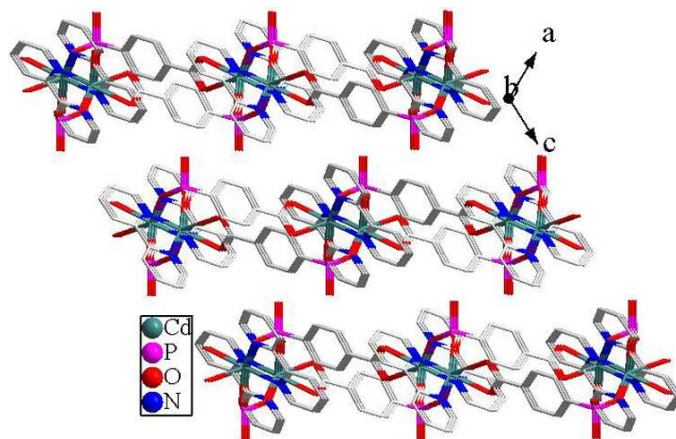


Fig. 6 View of the 2D layered structure of compound **2** along the *b*-axis. All H atoms are omitted for clarity.

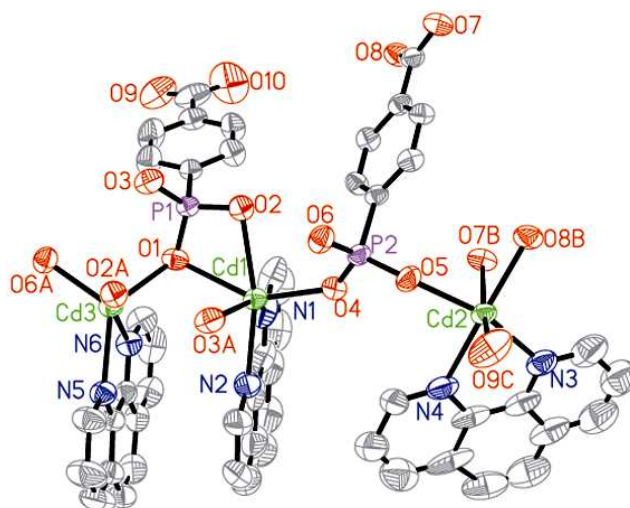


Fig. 7 Structure unit of compound **3** showing the atom labeling. Thermal ellipsoids are shown at the 50% probability level. All H atoms and lattice water molecules are omitted for clarity. Symmetry code for the generated atoms: A: $-x + 2, -y + 1, -z$; B: $-x + 1, -y, -z$; C: $x, y, z + 1$.

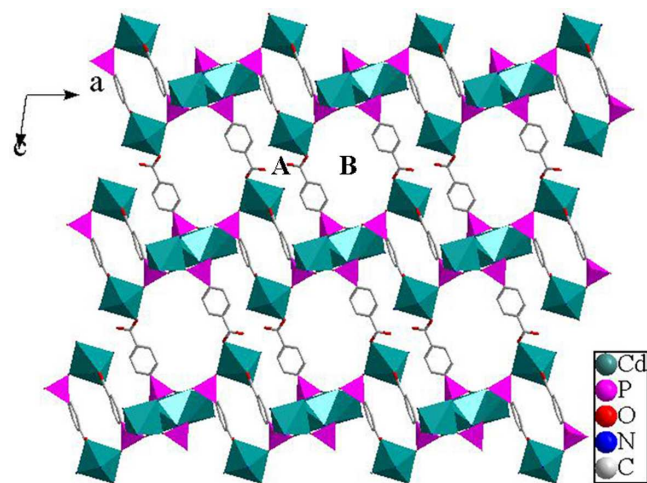


Fig. 8 A Polyhedral view of the two-dimensional inorganic layer of compound **3** in the *ac*-plane showing the windows in the structure. All C atoms of 1,10-phen ligands are omitted for clarity.

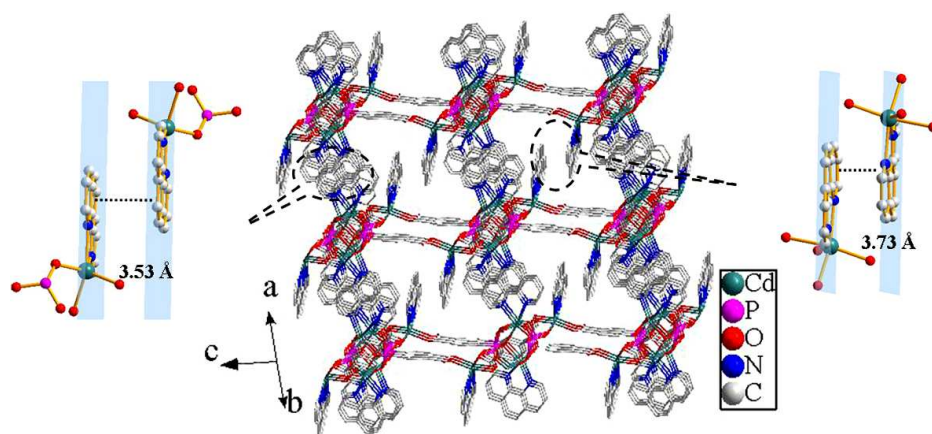


Fig. 9 View of the three-dimensional supramolecular structure *via* the π - π stacking interactions. The π - π stacking interactions between the adjacent 1,10-phen rings with the face-to-face distance of 3.53 and 3.73 Å.

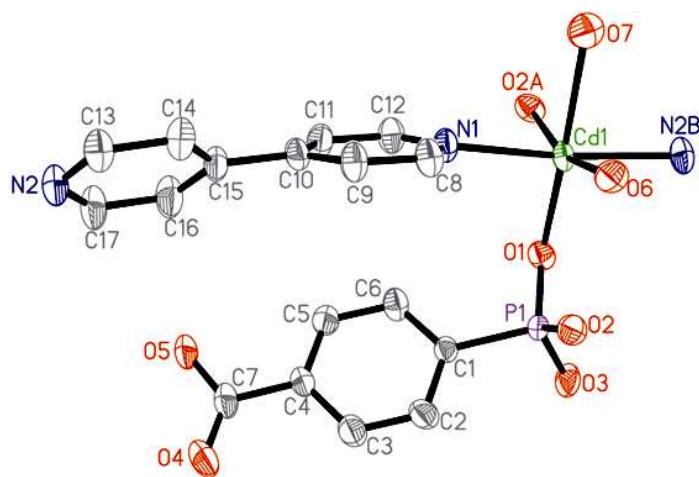


Fig. 10 Structure unit of compound **4** showing the atom labeling. Thermal ellipsoids are shown at the 50% probability level. All H atoms and lattice water molecules are omitted for clarity. Symmetry code for the generated atoms: A: $-x + 2, y + 1/2, -z + 1/2$; B: $x + 1, y, z$.

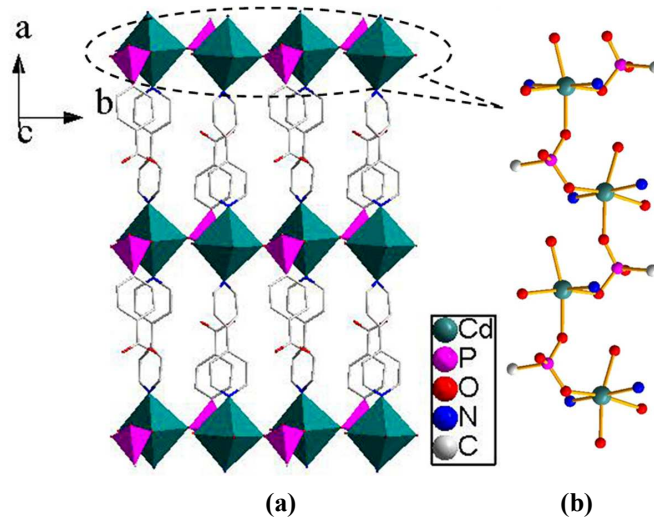


Fig. 11 (a) The layer structure of compound **4** viewed in ab -plane. Green polyhedra: CdO_4N_2 , pink tetrahedra: CPO_3 ; (b) A 1D chain of $\{\text{CdO}_6\}$ and $\{\text{CPO}_3\}$ polyhedra along the b -axis.

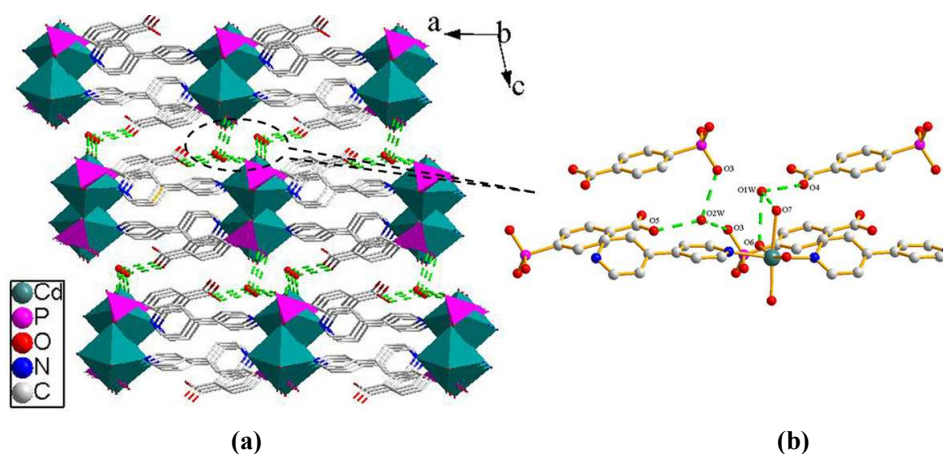


Fig. 12 (a) A polyhedral representation of the structure of compound **4** in the *ac*-plane. Green polyhedra: CdO_4N_2 , pink tetrahedra: CPO_3 ; (b) The connectivity of hydrogen bonds for compound **4**. All hydrogen atoms except for the hydrogen bonds are omitted for clarity.

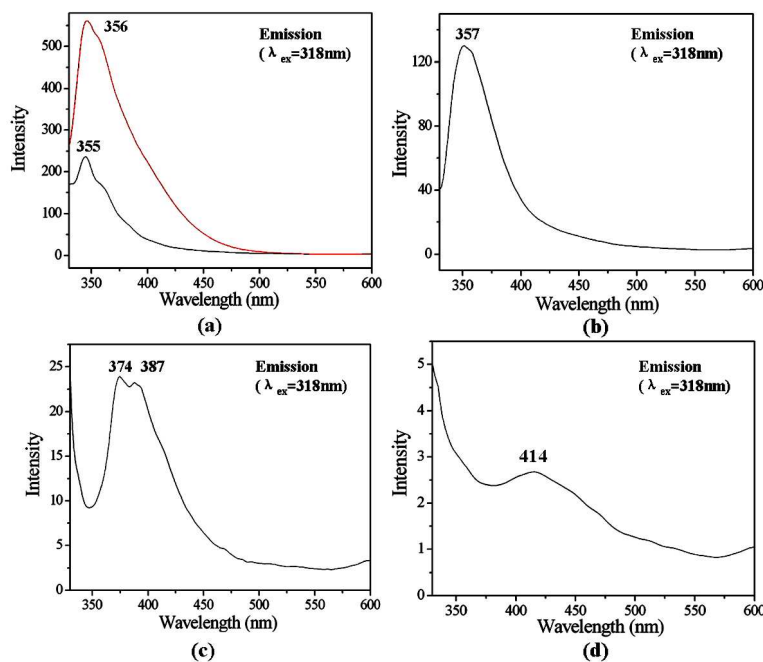


Fig. 13 (a) The comparison for the solid-state emission spectra of compound **1** (black line) and 4-cppH₃ (red line) at room temperature. (b) The comparison for the solid-state emission spectra of compound **2** at room temperature; (c) The comparison for the solid-state emission spectra of compound **3** at room temperature; (d) The comparison for the solid-state emission spectra of compound **4** at room temperature;

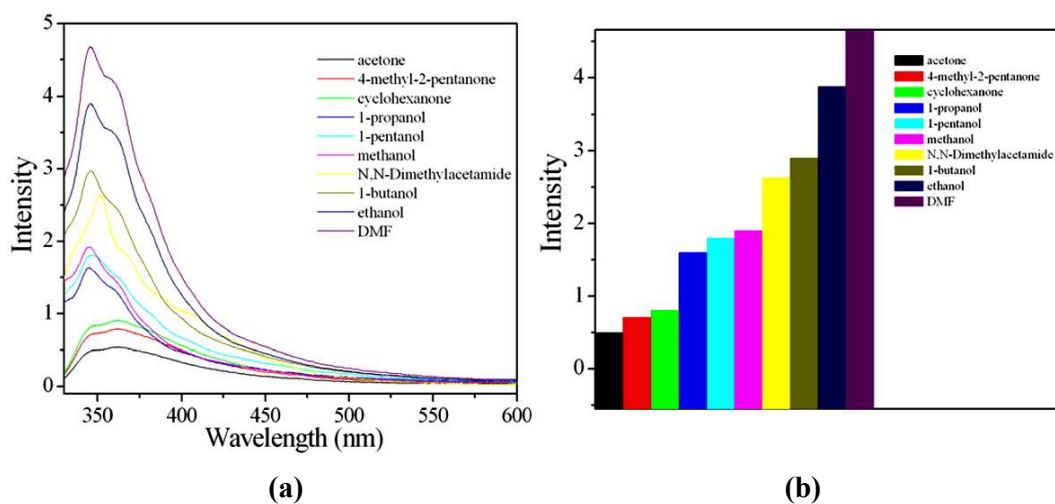


Fig. 14 (a) The emission spectra and (b) the transition intensities of compound **1** introduced into various pure solvents when excited at 318 nm.

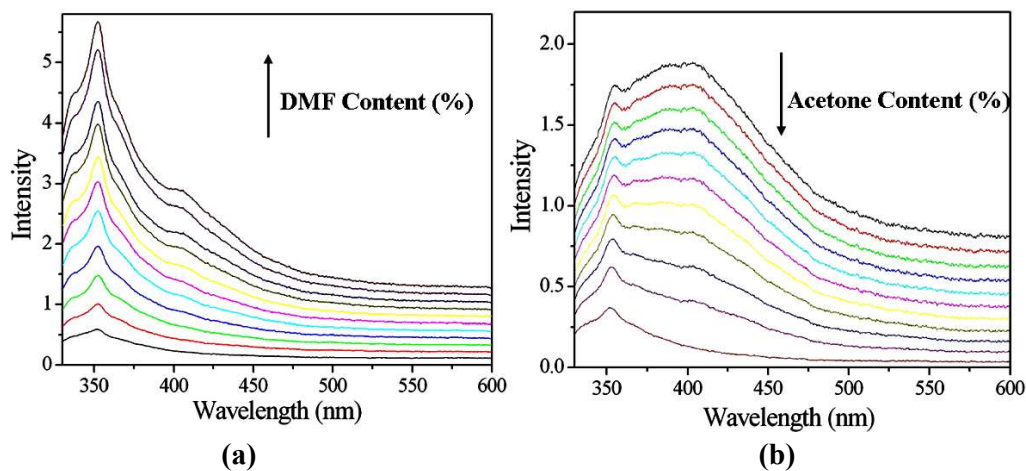
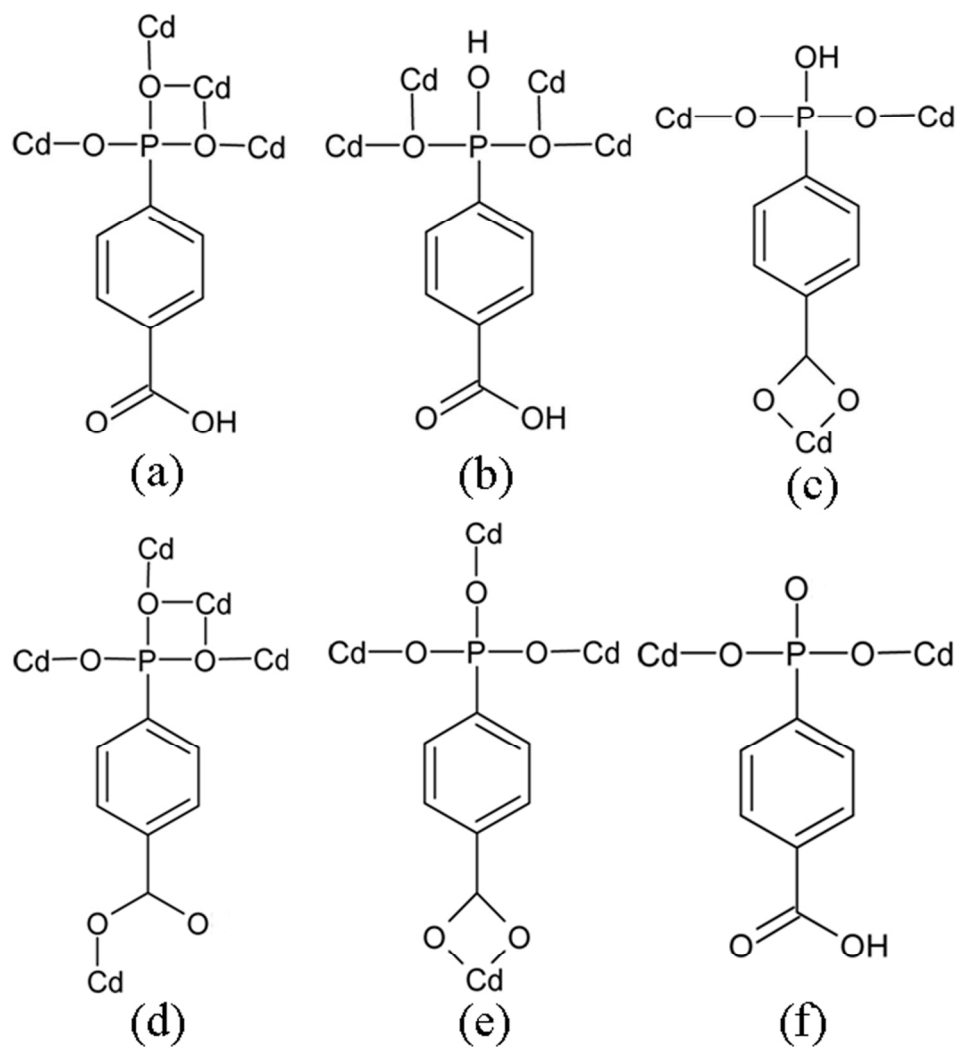
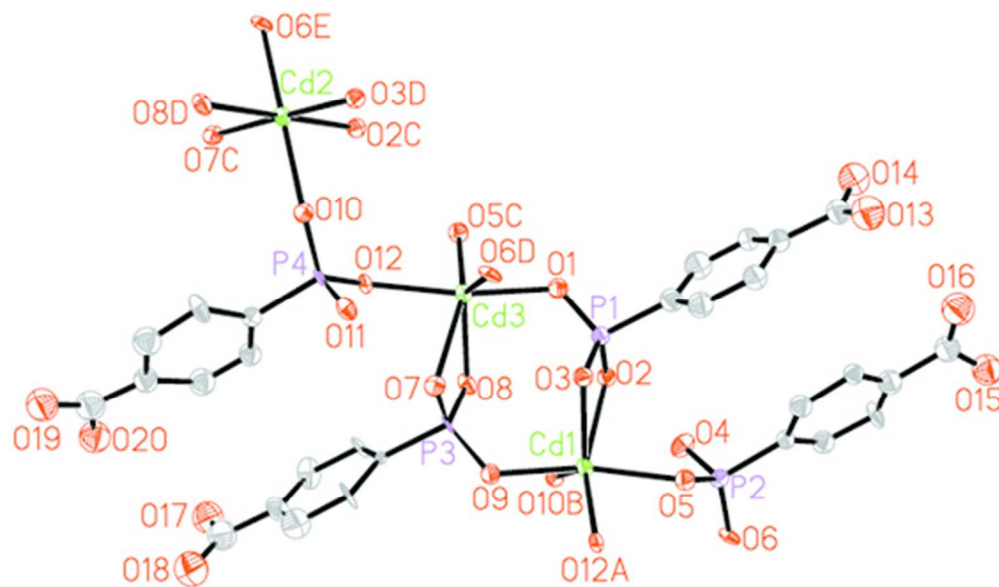


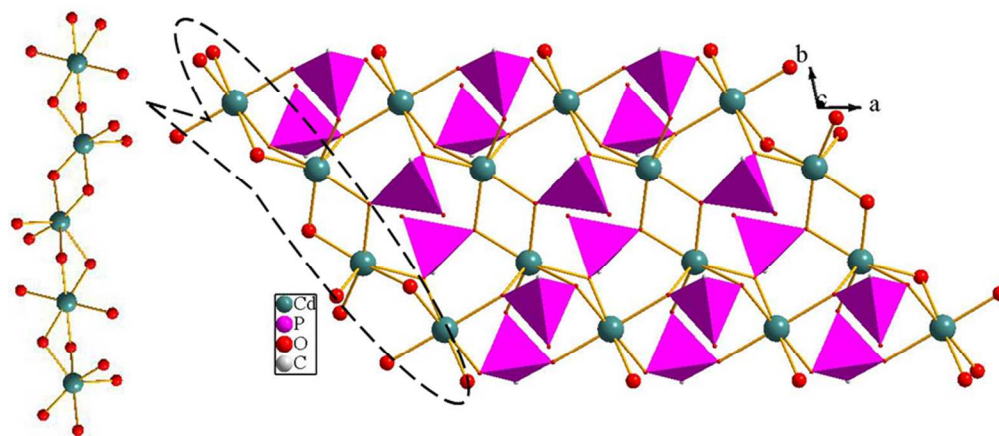
Fig. 15 The fluorescence properties of compound **1** emulsion in the presence of various contents of (a) DMF and (b) acetone solvent, respectively (by the frequency of 10 percent every time, from 0 percent to 100 percent).



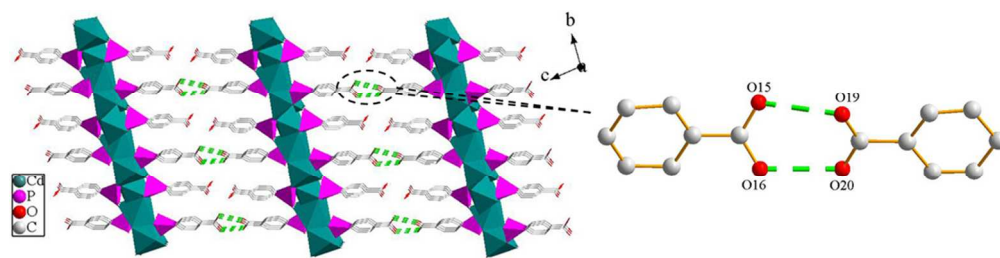
199x209mm (150 x 150 DPI)



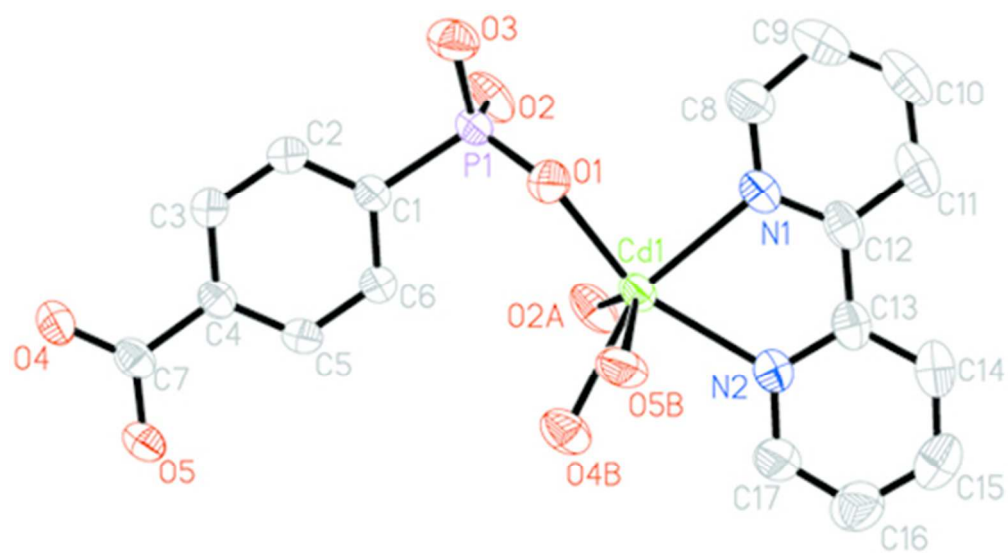
200x118mm (72 x 72 DPI)



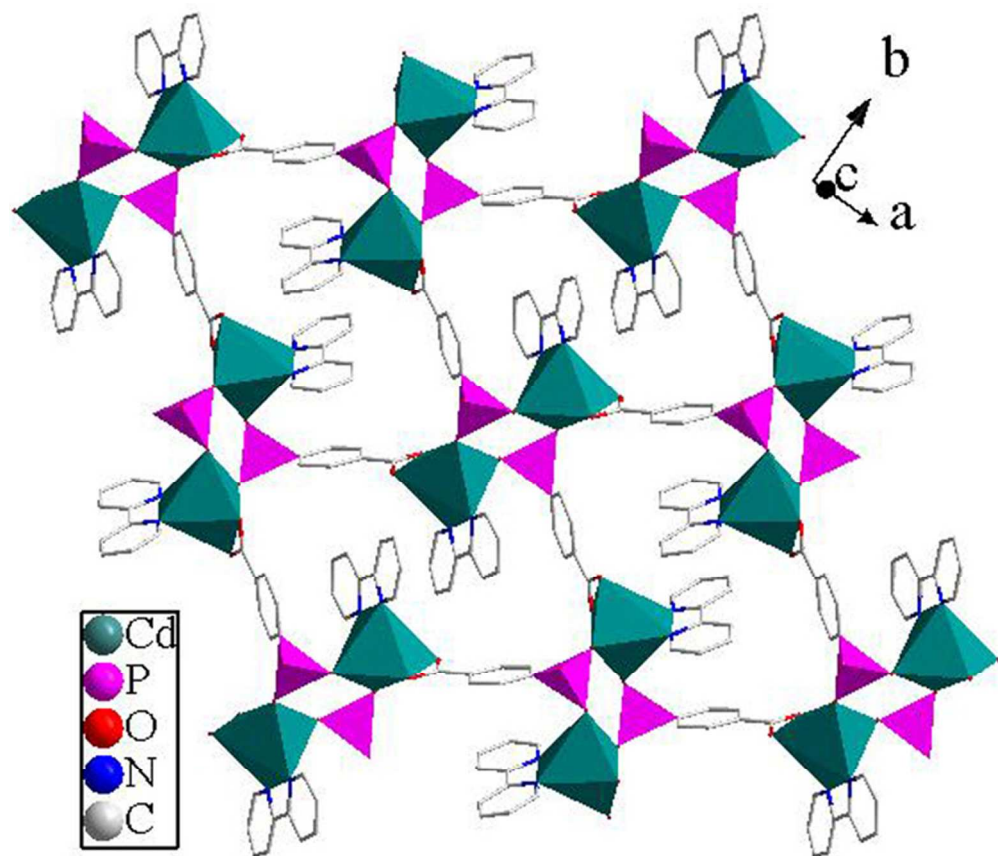
199x86mm (150 x 150 DPI)



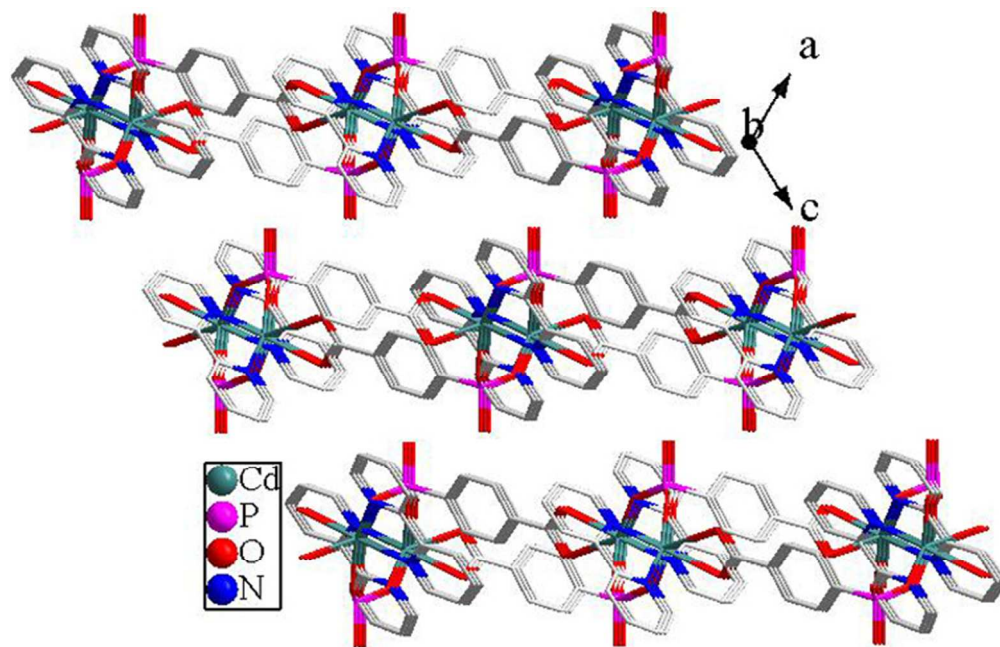
199x49mm (150 x 150 DPI)



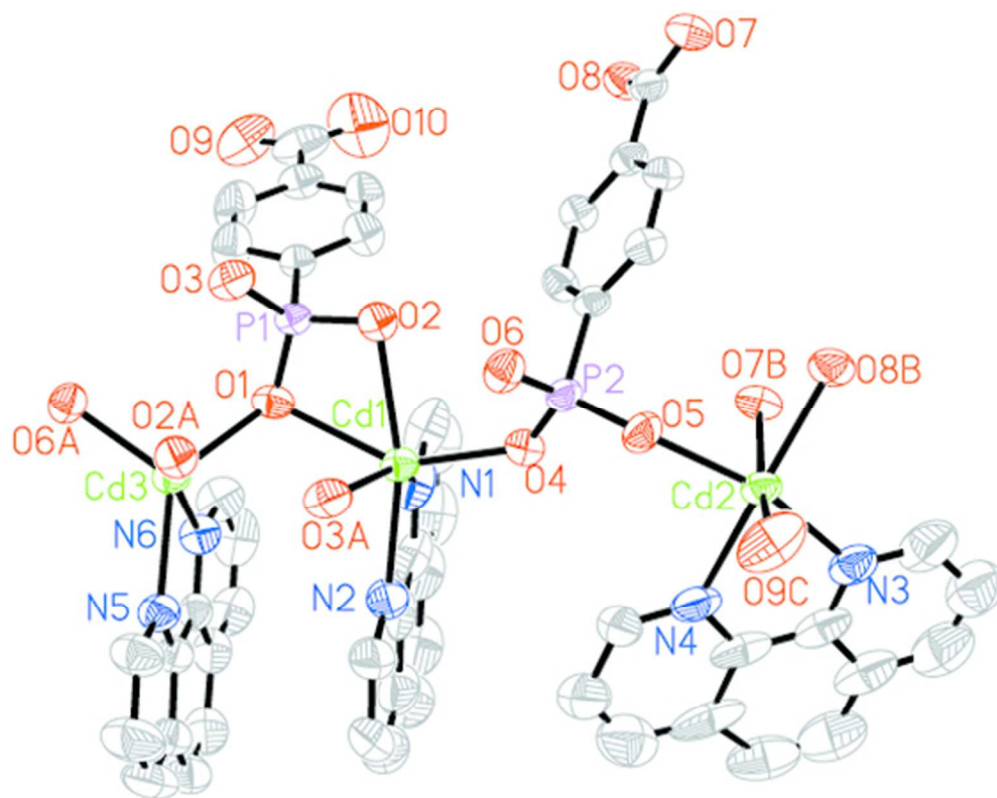
200x109mm (72 x 72 DPI)



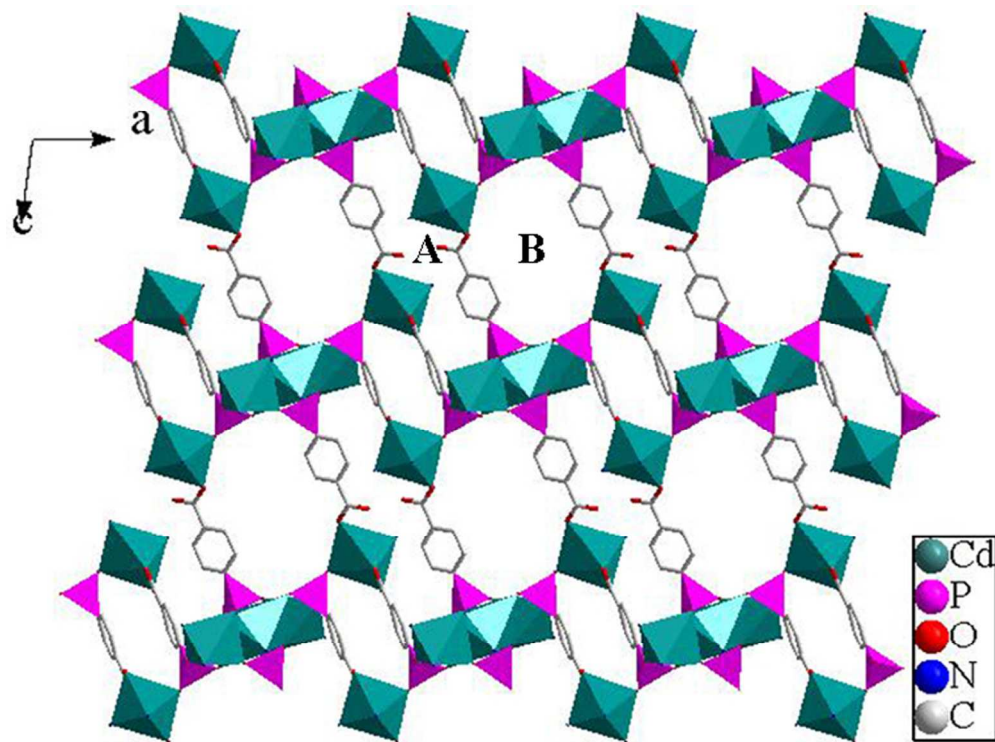
200x171mm (96 x 96 DPI)



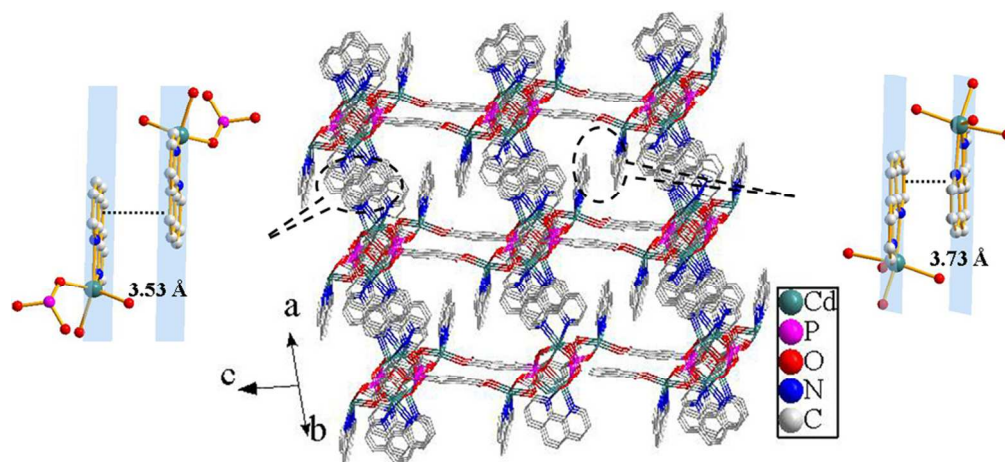
200x129mm (96 x 96 DPI)



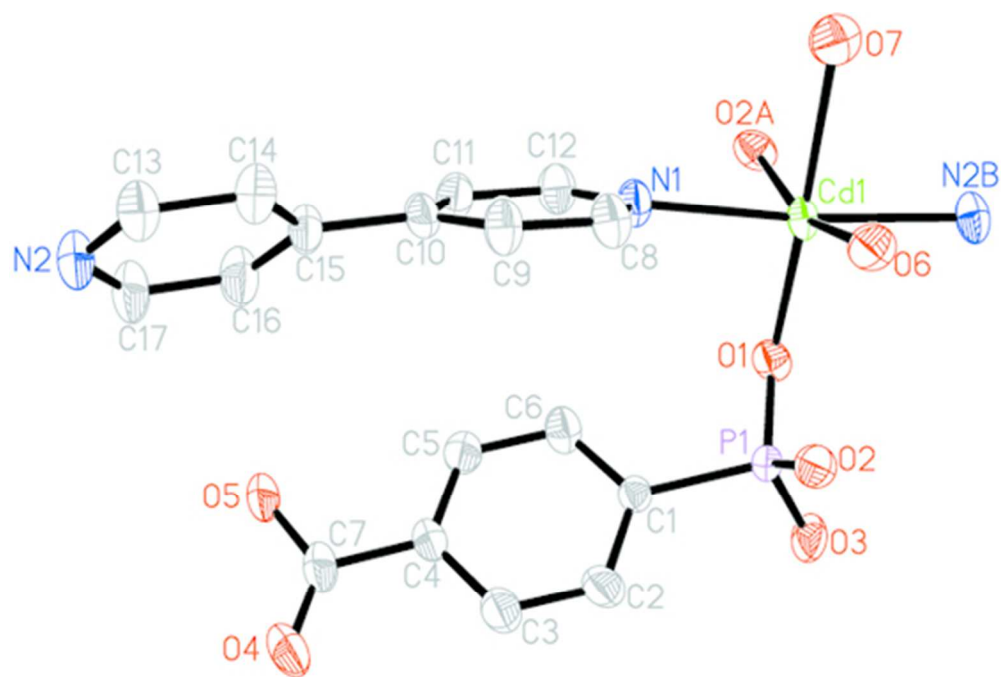
200x159mm (72 x 72 DPI)



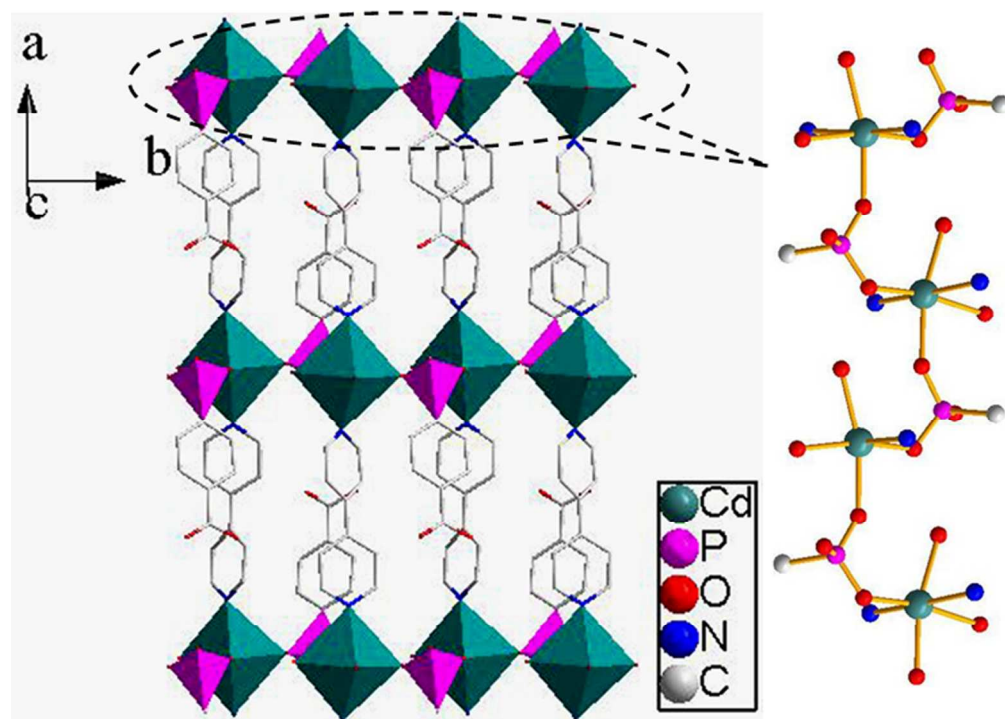
199x148mm (150 x 150 DPI)



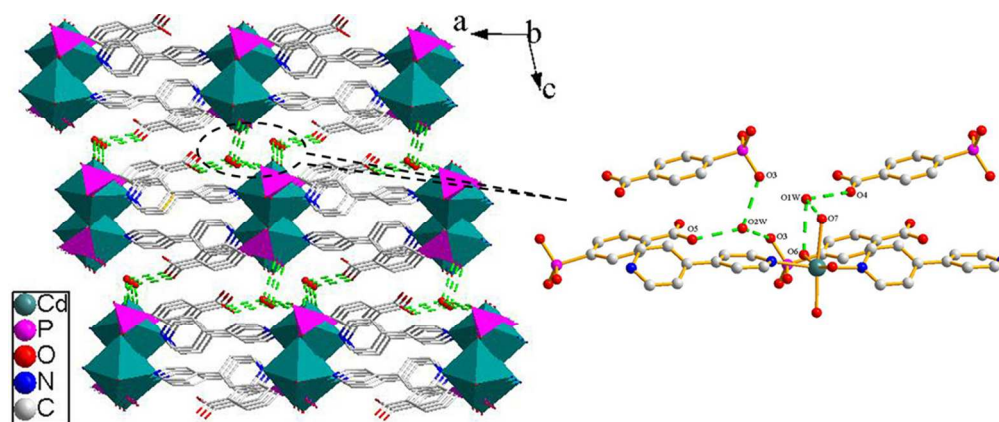
199x91mm (150 x 150 DPI)



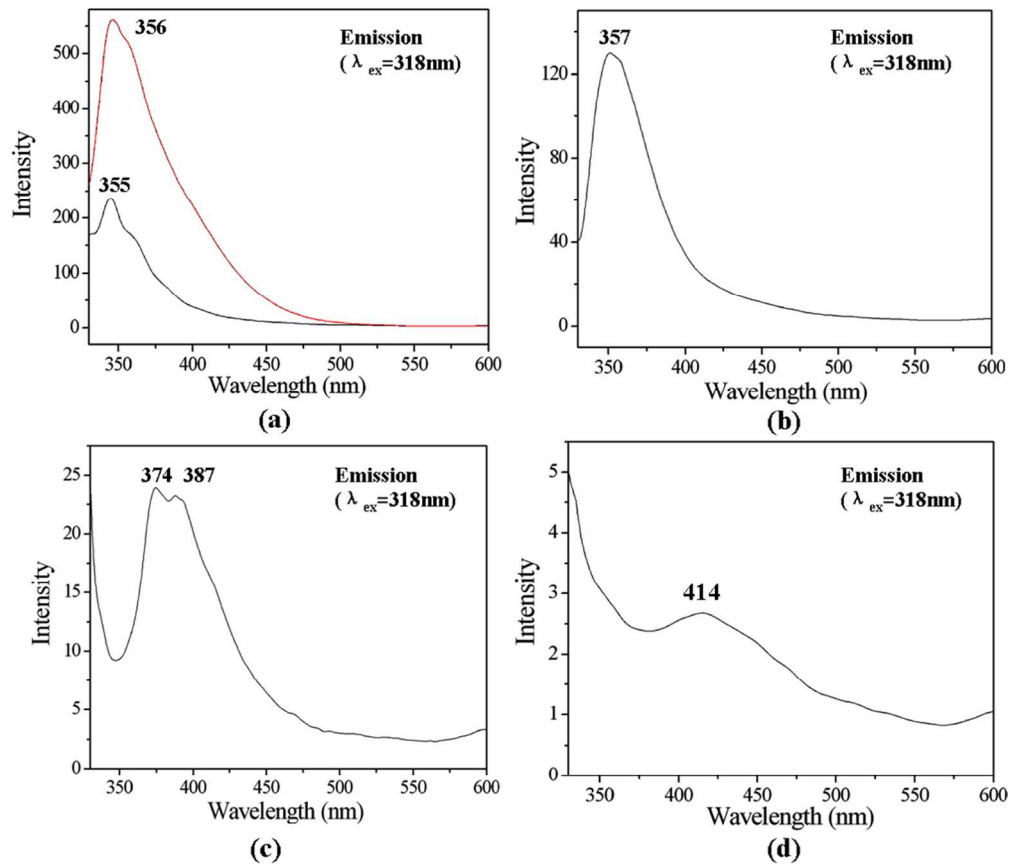
200x135mm (72 x 72 DPI)



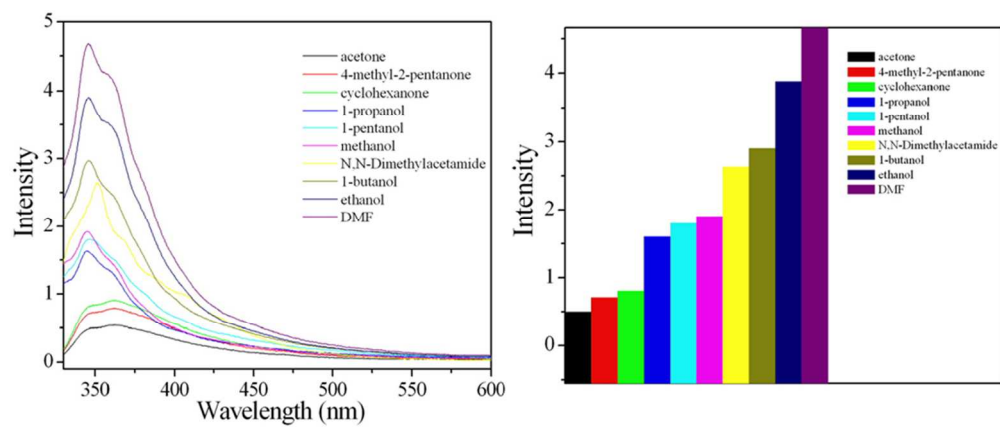
199x143mm (150 x 150 DPI)



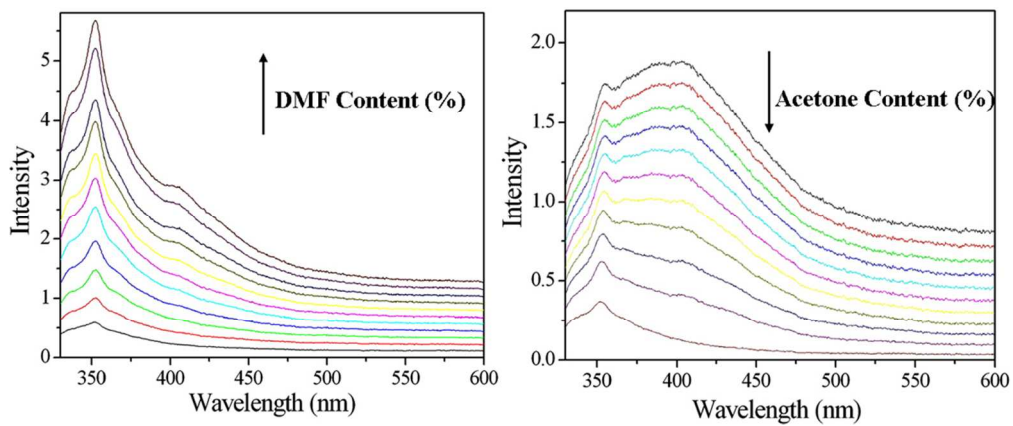
199x83mm (150 x 150 DPI)



199x172mm (150 x 150 DPI)



199x83mm (150 x 150 DPI)



199x83mm (150 x 150 DPI)

Table 1 Crystal data and structure refinement for compounds 1–4.

Compounds	1	2	3	4
Chemical formula	C ₂₈ H ₂₂ Cd ₃ O ₂₀ P ₄	C ₁₇ H ₁₇ CdN ₂ O ₇ P	C ₅₀ H ₄₄ Cd ₃ N ₆ O ₁₆ P ₂	C ₁₇ H ₂₁ CdN ₂ O ₉ P
Formula weight	1139.54	504.70	1384.05	540.73
Crystal system	Triclinic	Monoclinic	Triclinic	Monoclinic
Space group	<i>P</i> -1	<i>C</i> 2/ <i>c</i>	<i>P</i> -1	<i>P</i> 2(1)/ <i>c</i>
<i>a</i> / Å	5.6590(13)	18.2285(13)	13.9812(14)	11.7800(11)
<i>b</i> / Å	7.9562(18)	12.4643(9)	14.7218(14)	9.4034(9)
<i>c</i> / Å	19.147(4)	18.4247(19)	15.0185(14)	18.8322(18)
α (°)	96.620(3)	90	103.264(2)	90
β (°)	95.808(4)	117.2610(10)	92.471(2)	103.465(2)
γ (°)	98.313(3)	90	110.8650(10)	90
<i>V</i> (Å ³)	841.2(3)	3721.2(5)	2784.9(5)	2028.7(3)
<i>Z</i>	1	8	2	4
<i>D</i> _c / g·cm ⁻³	2.249	1.802	1.651	1.770
μ / mm ⁻¹	2.159	1.303	1.264	1.209
GOF on <i>F</i> ²	1.073	1.021	1.038	1.032
<i>R</i> , <i>R</i> _w [<i>I</i> > 2 σ (<i>I</i>)]	0.0525, 0.1493	0.0275, 0.0647	0.0512, 0.1532	0.0418, 0.1053
<i>R</i> , <i>R</i> _w (all data)	0.0563, 0.1553	0.0396, 0.0701	0.0827, 0.1738	0.0653, 0.1177

$R_1 = \Sigma (|F_0| - |F_c|) / \Sigma |F_0|$, $wR_2 = [\Sigma w (|F_0| - |F_c|)^2 / \Sigma w F_0^2]^{1/2}$.

Table 2 Hydrogen bond distances (Å) and angles (°) for compounds **1** and **4**.

Compound 1				
D–H...A	D(D–H)/ Å	d(H...A)/ Å	D–H...A/ °	d(D...A)/ Å
O15–H15A...O19	0.85	1.87	167.7	2.71(2)
O20–H20A...O16	0.85	1.79	159.4	2.60(2)
Compound 4				
D–H...A	D(D–H)/ Å	d(H...A)/ Å	D–H...A/ °	d(D...A)/ Å
O(1W)–H(1WB)...O(4)	0.85	1.95	150.9	2.724(5)
O(7)–H(7B)...O(1W)	0.85	2.00	142.7	2.720(5)
O(1W)–H(1WA)...O(6)	0.85	2.17	129.1	2.786(5)
O(2W)–H(2WA)...O(3)	0.85	1.89	163.4	2.712(5)
O(2W)–H(2WC)...O(3)	0.85	2.05	156.8	2.847(6)
O(5)–H(5A)...O(2W)	0.85	1.72	162.6	2.548(5)

Graphical Abstract

Four new cadmium carboxyphosphonates with 2D layered and 3D supramolecular structure, namely, $\text{Cd}_3[(4\text{-cppH})_2(4\text{-cppH}_2)_2]$ (**1**), $\text{Cd}[(2,2'\text{-bipy})(4\text{-cppH})]$ (**2**), $[\text{Cd}_3(1,10\text{-phen})_3(4\text{-cpp})_2] \cdot 6\text{H}_2\text{O}$ (**3**) and $[\text{Cd}(4,4'\text{-bipy})(4\text{-cppH})(\text{H}_2\text{O})_2] \cdot 2\text{H}_2\text{O}$ (**4**) (4-cppH₃ = 4-carboxyphenylphosphonic acid, 2,2'-bipy = 2,2'-bipyridine, 1,10-phen = 1,10-phenanthroline and 4,4'-bipy = 4,4'-bipyridine), have been synthesized under hydrothermal conditions. In compound **1**, {Cd(1)O₆}, {Cd(2)O₆}, {Cd(3)O₆} and {CPO₃} polyhedra form a layer in *ab* plane *via* edge- and corner-sharing. Neighboring layers compose into a 3D supramolecular network by hydrogen bonding interactions. The structure of compound **2** shows a new layered structure, in which the interconnection of two {Cd(1)O₄N₂} and two {CPO₃} polyhedra *via* corner-sharing forms a tetranuclear cluster, and the so-built tetranuclear clusters are bridged by the phosphonate ligands into a 2D layer. For compound **3**, {Cd(1)O₄N₂}, {Cd(2)O₄N₂}, {Cd(3)O₃N₂} and {CPO₃} polyhedra are interconnected by carboxyphosphonate ligands to a 2D layer in *ac* plane. Then the adjacent layers are further assembled into a 3D supramolecular structure through π - π stacking interactions. Cd(II) ions in compound **4** are bridged by 4,4'-bipy molecules into layers in *ab* plane. These layers are held together by hydrogen bonds into a 3D supramolecular structure. The thermal stabilities and luminescence properties of compounds **1**–**4** have been investigated. Interestingly, compound **1** is selective and reversible for sensing of DMF and acetone.

